OSCILLATOR MODELING AND PHASE NOISE

by

Brian Nguyen Limketkai

Memorandum No. UCB/ERL M04/14

20 May 2004

OSCILLATOR MODELING AND PHASE NOISE

by

Brian Nguyen Limketkai

Memorandum No. UCB/ERL M04/14

20 May 2004

ELECTRONICS RESEARCH LABORATORY

College of Engineering
University of California, Berkeley
94720

Oscillator Modeling and Phase Noise

by

Brian Nguyen Limketkai

B.S. (California Institute of Technology) 1998
M.S. (University of California, Berkeley) 1999

A dissertation submitted in partial satisfaction of the

requirements for the degree of

Doctor of Philosophy

in

Engineering-Electrical Engineering and Computer Sciences

in the

GRADUATE DIVISION

of the

UNIVERSITY OF CALIFORNIA, BERKELEY

Committee in charge:
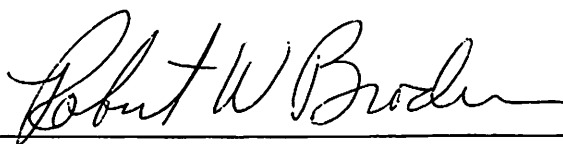Professor Robert W. Brodersen, Chair
Professor Robert G. Meyer
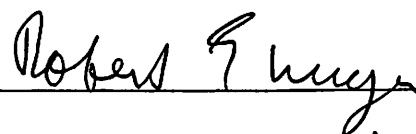Professor John C. Neu

Spring 2004

The dissertation of Brian Nguyen Limketkai is approved:

_____ 5/20/04

Chair   Date

_____ 5/19/04

                                         Date

_____ 05\19\04

                                         Date

University of California, Berkeley

Spring 2004

Oscillator Modeling and Phase Noise

© 2004

by

Brian Nguyen Limketkai

Abstract

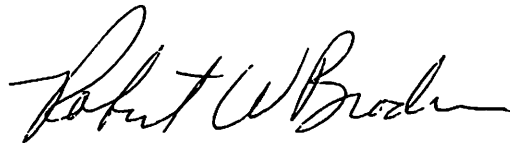Oscillator Modeling and Phase Noise

by

Brian Nguyen Limketkai

Doctor of Philosophy in Engineering-Electrical Engineering and Computer Sciences

University of California, Berkeley

Professor Robert W. Brodersen, Chair

Using a dynamical systems perspective, we develop a method to calculate phase noise in oscillators based on a particle diffusion model. Starting from the basic non-linear equations of motion, a phase diffusion equation is formulated by viewing the system in state space. The resulting phase diffusion solution is then found approximately by using multiple scale perturbation theory to get closed-form analytical expressions. In this way, the effects of the nonlinearities on the phase diffusion become evident. Similar techniques are then also applied to finding the locking bandwidth of a 2:1 injection-locked frequency divider.

Robert W. Brodersen, Chair

1

To my loving parents

who have stood behind me every step of the way,

Benito and Thanh-Nhan Lim

Contents

Figures

Preface

I once came across a UNIX fortune that read: "To understand physics, one simply has to understand the harmonic oscillator." Now although an obvious simplification, this quote underscores the importance of the role that oscillators play in most of science and engineering. Why is it so important? Perhaps it's because oscillators provide us with order through their repeating patterns. However, regardless of the philosophical reasons for their ubiquity, oscillators are here and can be found in almost all fields of study. In physics, we learn about them early on as the generator of waves, from acoustic to electromagnetic, or even of the quantum electron variety. In mechanics, they represent systems with springs that bounce up and down. In biology, our hearts beat with some period. A more interesting biological oscillation would be our sleep-wake cycle which has a period of about 24 hours. In optics, lasers are optical oscillators. In economics, it's the fluctuation of prices or perhaps the stock market. Finally, in electronics, oscillators are used to generate specific frequencies to regulate systems or create electromagnetic radiation. Clearly, the use of oscillators everywhere increases the value of understanding how they work.

Without being too rigorous on the definition of an oscillator, we note that most oscillators share certain characteristics. First and foremost, oscillators have a defined frequency of operation. Other properties may well be considered second-order in relation to this one trait, for it is this which defines the repetition or oscillation. This being obvious, we now introduce the more interesting second-order characteristics,

such as limiting amplitude, phase noise, and jitter. The limiting amplitude, as its name implies, is the strength of the oscillation. This is usually caused by nonlinearities in a self-sustained oscillator. Phase noise and jitter are two representations of noise in a non-ideal oscillator. Basically, they are caused by random fluctuations which disturb the oscillator's natural rhythm leading to variations in the oscillation frequency or period, respectively. These three second-order characteristics are present in almost all nonlinear oscillators, regardless of the application. Hence, their study will form the bulk of this thesis.

Exploring the nonlinear properties of oscillators is of great importance because rarely is an oscillator ever truly linear. The linear harmonic oscillator does not possess the capability to hold self-sustained oscillations. The oscillation amplitude in such systems depends on the initial conditions. Linear oscillators with negative damping may result in growth of oscillation amplitude, but this growth remains unchecked and will continue ad infinitum. A nonlinear oscillator, on the other hand, usually has a limiting amplitude which the oscillator will tend to, regardless of whether the initial conditions place the system at a point of lower or higher amplitude. The small nonlinearities present in real oscillators will eventually limit oscillation growth, resulting in the final amplitude of oscillation. For this reason, our study focuses on this class of oscillators.

Fortunately, nonlinear oscillators also allow for more interesting phenomena which do not manifest in linear oscillators. One example is frequency entrainment. Frequency entrainment, or injection-locking as it is sometimes called, is the ability of one nonlinear oscillator to couple or synchronize itself with another oscillation. This coupling results in both oscillations occuring at the same frequency, or rational multiples of each other. The latter being called superharmonic or subharmonic entrainment,

depending on whether the main oscillator's frequency is an integral multiple higher or lower than the external oscillation, respectively. Our study of nonlinear oscillators will include frequency entrainment as used in frequency dividers.

That being said, one may wonder what's wrong with the current answers out there. In the area of phase noise, a plethora of theories and methods exist to explain the mechanisms and calculations [30], [25] [26] [28] [29]. What are their faults?

Some of them [30] are basically curve fit methods which have a "fudge" factor to fit the data to measurements. This would not be very useful to providing additional insight into the design problem. Others [25] [26] try to add more intuitive explanations for the generation of phase noise, while detailing mathematical steps needed to arrive at a curve. These fall short however in providing a rigorous derivation of the phase noise spectrum starting from first principles. They start with an assumption on how noise gets transferred (multiply by transfer function) without really verifying as to whether one can still do this in a nonlinear system. Although [26] does consider a *linear* time-varying system, knowing whether nonlinear oscillators can be modeled by LTV systems has not been argued except through some simulations. Others [28] still have tried to provide a more foundational approach to tackling the phase noise problem by considering a particle diffusion model, similar to the approach considered in this thesis. However, the work stopped at the linear oscillator problem. To be fair, the author only wanted to present the gist of how phase noise could be generated. Perhaps the most rigorous of all the existing models is given in [29]. The mathematical machinery involved here, however, is complex. We do not imply that advanced mathematics should be avoided at all costs, since the approach taken seems similar to the one presented in this thesis. However, some of the results found in this thesis were not evident in the other work because of the different physical model used to

explain phase noise. The equations may be the same (Fokker-Planck), but the mental picture wasn't.

The main focus of this thesis is the development of methods to calculating phase noise and jitter in oscillators using a particle diffusion model. Starting from the basic equation for a nonlinear oscillator, we formulate the phase diffusion equations using perturbation theory and find solutions describing the evolution of the oscillator. The analytical solutions to the phase diffusion problem are shown and then applied to some simple models resulting in expressions for phase noise in terms of circuit components. This gives the theory a more applied flavor without sacrificing the foundational rigor. Although somewhat lengthy, Chapter 1 is considered the meat of this work, and for that reason alone, should not be skipped.

Incidentally, the use of perturbation theory to solving systems that evolve over time is not new. It is part of a growing field called dynamical systems theory (a merging of linear and nonlinear systems theory). Perturbation theory is often used to solve hard solutions which are "close" to known easy solutions. By expanding about the known solution, the hard solution can be approximately solved *analytically!*

Returning to the problem of injection-locking, we find that this topic has also been studied, though mainly from a linear point of view [35] [33]. However, nonlinear methods [23] [11] [16] from which this work was based on, do exist. We simply try to apply it to a circuit divider. Applying similar methods to those employed in the first chapter, we seek perturbation solutions to find how 2:1 frequency entrainment (2:1 injection-locking) can occur. Thus, Chapter 2 describes the use of subharmonic entrainment in an injection-locked frequency divider. Although treated in a noiseless fashion, similar mathematical methods are employed to demonstrate the benefits of the dynamical view of oscillators to solving problems.

Acknowledgments

Endeavoring to follow through a complete doctoral research project is not a feat which can easily be accomplished by only one person, at least not by me. My path from start to finish has been littered with obstacles over the past 6 years; and if it weren't for the kind help of certain good samaritans, I would not have gotten to where I stand now.

First, I would like to thank my dissertation committee for taking their time to read over my manuscript, dense, illegible, boring as it may be. They would be my advisor, Bob Brodersen, along with another great circuits professor, Bob Meyer, and a great math professor, John Neu.

Special thanks go out to advisor Bob for putting up with my stubbornness and letting me do research of a more mathematical nature. He kept me grounded when I tended to drift and go off on research tangents that consume me completely. Because of his pull, I was able to focus my efforts on a somewhat coherent thesis, which would otherwise have been a very noisy bit of scratch paper.

I also thank John Neu greatly for sharing his deep insight into perturbation theory with me, and for guiding me as I plodded through a lot of the derivations for phase noise. Without him, this would have been a 60 year PhD project. He also bought me many cups of coffee over the years.

But a PhD is not only about academics. There were many people who helped keep me insane during my first years in grad school.

There is Dennis Yee, a good friend and colleague who was the RF group leader at the time I joined. He showed me how senior grad students were supposed to glare at new students in order to maintain respect. If it weren't for him, I would have degenerated into your typical smiley grad student and lost my individuality.

In my age group, there were Ian O'Donnell, Chinh Doan, Sayf Alalusi, Johan Vanderhaegen, and David Sobel. These guys have been around since the very beginning of my graduate career. Ian showed me how much fun it was to ride a bike for long hours at a time while getting flipped off by a guy in a pickup truck riding around Lake Tahoe. That's an experience worth remembering. Chinh was a main source of distraction. We spent countless hours playing pool and racing to see who had the most checked-out library books—I won (the book contest, that is). Sayf and I pioneered center jousting with knock-off razor scooters and plastic swords. Johan and I have had many great discussions on computers and programming. If it weren't for him, how would I have been able to waste my time on micromanaging my computer? Dave was very good at constantly reminding me about how hard-working I was whenever he went to see a talk.

And the list doesn't end there. I also thank Ada Poon for being very nice by reminding me about important up and coming events, like what to do by when to get my thesis filed, or other things I tend to overlook. There's Henry Jen, a good friend who can discuss anything at enormous length, even beyond the point of boredom for most people. There is Jeff Gilbert, then a student who had an insatiable appetite for food and was always willing to grab something to eat with me. I tend to be hungrier these days. I also had the great opportunity to meet Sohrab Emami, an eclectic who likes to measure. This guy operates at a speed unfathomable by most human beings. I have to drink sake with him in order to understand what he's saying. I met Nate

Pletcher, cycliste extraordinaire. Nate, Ian, and I used to pretend like we were cycling together by setting up meeting times and missing them.

I also do thank Ning Zhang, Rhett Davis, and Mehul Shah for making my transition from a small school to a bigger school easier when I entered grad school.

Of course, there are people outside my group that deserve thanks, too. My friends from Caltech who crossed over the grapevine with me are Payam Pakzad, Vito Dai, Ben Miller, and Bret Victor. These guys are some of the best that Caltech has to offer. They provided me with many hours of great discussion on random topics from ergodic theory on Polish spaces to free energy codes. Although my understanding was very limited, they taught me key words which I can now use when I want to pretend to be smart.

I would also like to acknowledge the support from the people closest to me, for they were the ones who had the most effect on my well-being. My brothers, Berkeley, Benson, Benjie, and Benhan. My big brother Berkeley kept me very informed about the state of affairs in China. Benson just bothered me. Benjie bothered me even more! and Benhan never talked to me. Heh. :)

But they are the greatest brothers. I admit that without them, life itself would have been more boring. For that, I thank them all with my deepest gratitude for making the last couple of years, and the 20 years before that, enjoyable and an experience worth remembering.

I want to also thank Vicki for all of her support and wise decisions. Had she not stopped me, I might have boughten many things (and wasted all my money) on ebay. My grad student career would not have been the same without her.

But most of all, I thank my parents, Benito and Thanh-Nhan, for they were the ones who made me want to get a PhD in the first place. They believed in me the

most, even when I didn't. They were a source of continuous encouragement and love. They were definitely responsible for shaping me into the monster that I am today, and I thank them. This thesis is dedicated to my parents, and their parents, for they worked hard to instill values in my parents who trickled them down to me. Thank you mommy and daddy!

Chapter 1

Phase Noise and Jitter

1.1 Noise in oscillators

Phase noise and jitter are two views of the same kind of noise. When viewed in frequency space, the noise in an oscillator appears as "skirts" around a peak at one frequency, denoting variations in the frequency of oscillation. This is referred to as phase noise. When viewed in time, the noise appears as "fuzz" around the zero crossings when subsequent cycles are superimposed on top of each other, implying that the period of oscillation is not held steady at one fixed value. These variations are referred to as jitter. Because noise is often regarded as a nonideality, understanding these two quantities is of great importance to better designing low-noise oscillators.

The are two types of noise which we consider which give rise to oscillator phase noise: white noise and flicker noise. White noise, so called because of its flat power spectral density, is an uncorrelated noise process which disturbs the oscillator in such

a way that the phase noise takes on a $1/f^2$ dependence about the peak, where f is the offset frequency from the oscillator's natural frequency. In electronic oscillators, this may be due to thermal noise or shot noise in resistors or the active device. Flicker noise, on the other hand, is a correlated noise process which results in the phase noise taking a $1/f^3$ shape. Flicker noise comes mainly from transistors, although some resistors may also contribute. As this has been widely studied [4] [13] [14] [15], this work will not focus on the origins of flicker noise, but rather on the process of converting this noise into the form that it takes in the oscillator, namely the $1/f^3$ shape. We assume the charge-trapping explanation [4] [15] and use the autocorrelation function given by that theory in all calculations.

1.2   Analyzing phase noise

Although the overall $1/f^2$ shape of phase noise has been known for some time, calculating the exact values has been elusive. Many techniques and theories exist [30] [26] [28] [29]. Some of them are based on nonlinear techniques similar to the work presented here, but the majority are linear.

A linear analysis of phase noise is not appropriate because of the very nonlinear nature of oscillators. First of all, it is difficult to accurately calculate the limiting amplitude of an oscillator based solely on linear techniques because the limiting process is inherently nonlinear. Other nonlinearities which affect the transformation of white noise to the $1/f^2$ shape would also be neglected, resulting in a miscalculation of the value of phase noise. To cope with this inaccuracy, some have proposed an extension to these methods which rely on linear time-varying techniques. The basic gist is that noise gets transferred to the output differently, depending on where in the cycle of oscillation it gets injected. This information is captured by having time-varying

noise transfer functions from each source to the output. Although more accurate, this method relies upon the use of a circuit simulator to find the instantaneous transfer functions. In a way, this is sidestepping the issue of actually solving the nonlinear equations.

Past nonlinear analyses, on the other hand, have focused on exact solutions which led to very involved methods which are more suitable for simulators.

This work was motivated by the need to get accurate solutions for phase noise while still being able to use hand analysis. We can achieve this through the use of two major concepts. First, we realize that we can put the oscillator in a dynamical systems framework and view the evolution of the oscillator's state as a diffusion process, which will be described in detail in the following section. Second, we apply perturbation methods to solve the resulting partial differential equations. The use of perturbation theory to solve these equations enables us to calculate good approximate solutions by hand, essentially trading over the exactness of previous nonlinear analyses for analytical solvability, thereby giving us a powerful tool in our attempts at solving phase noise.

1.3   Phase space and flows

1.3.1   Phase space

This method of calculating phase noise and jitter is based on placing the oscillator in a dynamical systems framework. The system is viewed as having a state which evolves over time in some space, called the phase space or state space. The dimension of this space depends on the number of state variables needed to fully describe the system. In this work, we confine our oscillators to being within R^2. In oscillators where this is not true everywhere, we focus on the cases which allow us to approximate it as a

planar oscillation. The evolution of the state traces out a trajectory in phase space which we call a flow. This is a common way to view oscillators in a more mathematical setting and provides us with a means to finding phase noise.

1.3.2   Phase diffusion

One difficulty in calculating phase noise comes from the random nature of noise itself. Finding the power spectral density of a random path traced out in the phase space can be very challenging if one must consider all the possible paths that any sample oscillator may take. Consider Fig. 1.1a, which is one possible realization of a noisy oscillator's trajectory. The orbit is "jagged", as noise disturbs the otherwise smooth path of this oscillator's state. Solving for the properties, such as the phase noise or jitter, of the trajectories by considering how noise affects each realization (sample path) may be very involved. Another viewpoint to this problem is to consider the flow of the ensemble of oscillators, such as in Fig. 1.1b. In this case, we solve for the flow of the probability of the realized oscillator being in a specific state, or region of phase space. Solving for the density of realizable oscillators instead of the one

| (a) | (b) |
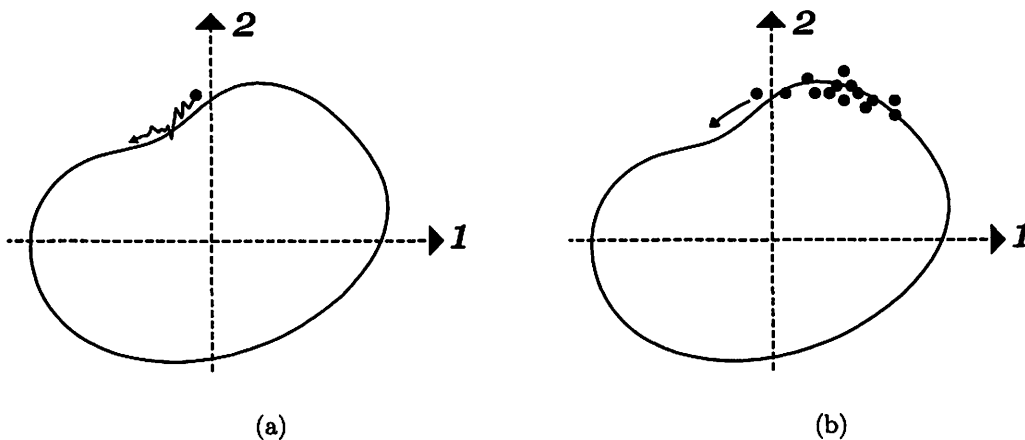
Figure 1.1   (a) one realization of the trajectory of a noisy oscillator. (b) flow of the ensemble of oscillators.

realized path transforms the problem into a more tractable problem. This way, we have converted our stochastic problem into a deterministic one, in which we can use ordinary calculus to solve. The resulting equation describing the flow of the density of oscillators is none other than the advection-diffusion equation

$$\eta_t + \nabla \cdot (\mathbf{u}\eta) = D\Delta\eta \tag{1.1}$$

where η is the probability density, $\mathbf{u}$ is the velocity field, and D is the diffusion constant. The advective or drift component of this equation handles the deterministic aspects of the system's evolution, describing the path in the noiseless case. The diffusive component models the random aspects as a flow of the ensemble. Derivations of the advection and diffusion equations can be found in the appendix.

1.4 Solving the phase diffusion equation

1.4.1 Phase noise

We only consider nearly sinusoidal oscillators with small nonlinearities and noise, described by the equation

$$\ddot{q} + q = \epsilon f(q, \dot{q}) + w(t) \tag{1.2}$$

where $\epsilon \ll 1$ is the small parameter and the noise, $w(t)$, is white and of $O(\epsilon)$. We will later make the assumption that the noise, $w(t)$, is asymptotically smaller than the nonlinearity to further reduce the problem; but for now, we treat them as being of the same order. Rewriting (1.2) as a system of equations, we get

$$\dot{q} = v$$
$$\dot{v} = -q + \epsilon f(q, v) + w(t) \tag{1.3}$$

5

The advection-diffusion (Fokker-Planck) equation for this system (derived in Appendix) is

$$\eta_t + \nabla \cdot ((v\mathbf{1} - q\mathbf{2})\eta + (\epsilon f(q,v)\eta - \epsilon D\eta_v)\mathbf{2}) = 0 \qquad (1.4)$$

where **1** is the unit vector in the q-direction, and **2** is the unit vector in the v-direction. We can rewrite (1.4) as

$$\eta_t + (v\mathbf{1} - q\mathbf{2}) \cdot \nabla\eta + \epsilon(f\eta)_v - \epsilon D\eta_{vv} = 0 \qquad (1.5)$$

Since our oscillator is almost sinusoidal, it would be best to study our system in polar coordinates. We start by relating the rectangular coordinates (q,v) to polar coordinates (r,θ), where $q = r\cos\theta$ and $v = r\sin\theta$. We get some relations for the partial derivatives,

$$
\begin{aligned}
\partial_q &= \cos\theta\,\partial_r &-&\quad \frac{1}{r}\sin\theta\,\partial_\theta \qquad & \partial_r &= \cos\theta\,\partial_q &+& \sin\theta\,\partial_v \\
\partial_v &= \sin\theta\,\partial_r &+&\quad \frac{1}{r}\cos\theta\,\partial_\theta \qquad & \partial_\theta &= -r\sin\theta\,\partial_q &+& r\cos\theta\,\partial_v
\end{aligned}
\qquad (1.6)
$$

and the unit vectors,

$$
\begin{aligned}
\mathbf{1} &= \cos\theta\,\mathbf{r} &-& \sin\theta\,\boldsymbol{\theta} \qquad & \mathbf{r} &= \cos\theta\,\mathbf{1} &+& \sin\theta\,\mathbf{2} \\
\mathbf{2} &= \sin\theta\,\mathbf{r} &+& \cos\theta\,\boldsymbol{\theta} \qquad & \boldsymbol{\theta} &= -\sin\theta\,\mathbf{1} &+& \cos\theta\,\mathbf{2}
\end{aligned}
\qquad (1.7)
$$

The advection-diffusion equation (1.5) becomes

$$\eta_t - \eta_\theta + \epsilon\left(\sin\theta\,\partial_r + \frac{1}{r}\cos\theta\,\partial_\theta\right)(f\eta) - \epsilon D\left(\sin\theta\,\partial_r + \frac{1}{r}\cos\theta\,\partial_\theta\right)^2\eta = 0 \qquad (1.8)$$

where we used

$$\nabla\eta = \eta_r\,\mathbf{r} + \frac{1}{r}\eta_\theta\,\boldsymbol{\theta} \qquad (1.9)$$

as the gradient in polar coordinates.

Setting $\epsilon = 0$ in (1.8), we get the zeroth-order equation

$$\eta_t - \eta_\theta = 0 \qquad (1.10)$$

which is just the equation of a simple harmonic oscillator. We see that η is only a function of $(t + \theta)$. This is consistent with the phase decreasing linearly with time as the oscillator's state moves clockwise around a circle. This motivates an expansion about a rotating frame of angular speed 1. We convert to a rotating frame by defining a new variable $\phi = \theta + t$. In this rotating frame, our leading order solution will be made to be independent of time, t, and depend only on ϕ. Our advection-diffusion equation in this new frame is

$$\eta_t + \epsilon \left(sin(\phi - t)\partial_r + \frac{1}{r}\cos(\phi - t)\partial_\phi \right)(f\eta)$$

$$- \epsilon D \left(\sin(\phi - t)\partial_r + \frac{1}{r}\cos(\phi - t)\partial_\phi \right)^2 \eta = 0 \qquad (1.11)$$

To accomodate the change in the oscillator due to small perturbations from noise and the nonlinearity, we introduce another time scale, $T \equiv \epsilon t$, called *slow* time. By creating the slow time variable, we are essentially separating the effects that occur on a slower time scale from the fast oscillations. The *fast* time variable, t, is responsible for effects that occur on the order of the period. This separation allows us to focus on the phase diffusion. Our zeroth-order solution, η^0, will depend on T, as will all other terms in our perturbation expansion. Thus, we use the perturbation expansion

$$\eta(r, \phi, t, T) = \eta^0(r, \phi, T) + \epsilon \eta^1(r, \phi, t, T) + \ldots \qquad (1.12)$$

We choose to make our solution, η, 2π-periodic in the fast time variable, t. Slow changes in the system will be handled by modulating the solution via the slow time variable, T. Applying the perturbation expansion (1.12) to (1.11) and collecting terms of $O(\epsilon)$, we find

$$\eta_T^0 + \eta_t^1 + \left(\sin(\phi - t)\,\partial_r + \frac{1}{r}\cos(\phi - t)\,\partial_\phi \right)(f\eta^0)$$

$$- D \left(\sin(\phi - t)\,\partial_r + \frac{1}{r}\cos(\phi - t)\,\partial_\phi \right)^2 \eta^0 = 0 \qquad (1.13)$$

Noting that η is periodic in t, we integrate (1.13) over $[0, 2\pi]$ to get

$$\int_0^{2\pi} \eta_T^0 \, dt + \int_0^{2\pi} \eta_t^1 \, dt \tag{1.14}$$

$$+ \int_0^{2\pi} \sin(\phi - t)\partial_r(f\eta^0) \, dt \tag{1.15}$$

$$+ \int_0^{2\pi} \frac{1}{r} \cos(\phi - t)\partial_\phi(f\eta^0) \, dt \tag{1.16}$$

$$- D \int_0^{2\pi} \left(\sin(\phi - t)\partial_r + \frac{1}{r}\cos(\phi - t)\partial_\phi \right)^2 \eta^0 \, dt = 0 \tag{1.17}$$

We now focus on each of the terms (1.14)–(1.17).

Term (1.14)

$$\int_0^{2\pi} \eta_T^0 \, dt + \int_0^{2\pi} \eta_t^1 \, dt = 2\pi\eta_T^0 + \left[\eta^1\right]_0^{2\pi} \tag{1.18}$$

$$= 2\pi\eta_T^0 \tag{1.19}$$

since η^0 is independent of t, and η^1 is 2π-periodic in t.

Term (1.15)

$$\int_0^{2\pi} \sin(\phi - t)\partial_r(f\eta^0) \, dt = \partial_r \left(\eta^0 \int_0^{2\pi} f \sin(\phi - t) \, dt \right) \tag{1.20}$$

$$= \partial_r \left(\eta^0 \int_0^{2\pi} f \sin\theta \, d\theta \right) \tag{1.21}$$

$$= 2\pi\partial_r \left(U\eta^0 \right) \tag{1.22}$$

where we made the definition

$$U = \frac{1}{2\pi} \int_0^{2\pi} f \sin\theta \, d\theta \tag{1.23}$$

Term (1.16)

$$\int_0^{2\pi} \frac{1}{r}\cos(\phi - t)\partial_\phi(f\eta^0) \, dt = \frac{\eta^0}{r} \int_0^{2\pi} \cos(\phi - t) f_\phi \, dt + \frac{\eta_\phi^0}{r} \int_0^{2\pi} f \cos(\phi - t) \, dt \tag{1.24}$$

$$= \frac{\eta^0}{r} \int_0^{2\pi} f \sin(\phi - t)\, dt + \frac{\eta_\phi^0}{r} \int_0^{2\pi} f \cos(\phi - t)\, dt \quad (1.25)$$

$$= \frac{\eta^0}{r} \int_0^{2\pi} f \sin\theta\, d\theta + \frac{\eta_\phi^0}{r} \int_0^{2\pi} f \cos\theta\, d\theta \quad (1.26)$$

$$= 2\pi \frac{\eta^0}{r} U + 2\pi \frac{\eta_\phi^0}{r} V \quad (1.27)$$

where we used integration by parts to get from (1.24) to (1.25) (note that $f_\phi = -f_t$), and, in addition to (1.23), we defined another integral

$$V = \frac{1}{2\pi} \int_0^{2\pi} f \cos\theta\, d\theta \quad (1.28)$$

Term (1.17)

$$I = \int_0^{2\pi} \left(\sin(\phi - t)\partial_r + \frac{1}{r}\cos(\phi - t)\partial_\phi \right)^2 \eta^0\, dt \quad (1.29)$$

$$= \int_0^{2\pi} \sin^2(\phi - t)\eta_{rr}^0\, dt$$

$$+ \int_0^{2\pi} \sin(\phi - t)\cos(\phi - t)\partial_r\left(\frac{\eta_\phi^0}{r}\right)\, dt$$

$$+ \int_0^{2\pi} \frac{1}{r}\cos(\phi - t)\partial_\phi(\sin(\phi - t)\eta_r^0)\, dt$$

$$+ \int_0^{2\pi} \frac{1}{r^2}\cos(\phi - t)\partial_\phi(\cos(\phi - t)\eta_\phi^0)\, dt \quad (1.30)$$

$$= \pi\eta_{rr}^0 + \frac{1}{r}\int_0^{2\pi} \cos^2(\phi - t)\eta_r^0\, dt + \frac{1}{r^2}\int_0^{2\pi} \cos^2(\phi - t)\eta_{\phi\phi}^0\, dt \quad (1.31)$$

$$= \pi\eta_{rr}^0 + \frac{\pi}{r}\eta_r^0 + \frac{\pi}{r^2}\eta_{\phi\phi}^0 \quad (1.32)$$

Thus, combining (1.19),(1.22),(1.27), and (1.32), we get the expression for the reduced advection-diffusion equation describing the leading order behavior

$$\eta_T^0 + \frac{1}{r}\partial_r(rU\eta^0) + \frac{\eta_\phi^0}{r}V = \frac{D}{2}\Delta\eta^0 \quad (1.33)$$

where we used the definition for the Laplacian

$$\Delta \equiv \partial_{rr} + \frac{1}{r}\partial_r + \frac{1}{r^2}\partial_{\phi\phi} \quad (1.34)$$

Note how although the initial diffusion in (1.4) occurs only in one direction (upward in the v-direction), the diffusion in (1.33) is isotropic. This is because we converted to the rotating frame, where the v-direction vector is now rotating.

We now rewrite (1.33) into a form which makes the advective component explicit to see how trajectories flow in this rotating frame.

$$\frac{D}{2}\Delta\eta^0 = \eta_T^0 + \frac{1}{r}\left(\partial_r(rU\eta^0) + \frac{1}{r}\partial_\phi(rV\eta^0)\right) \tag{1.35}$$

$$\approx \eta_T^0 + \frac{1}{r_c}\nabla\cdot(rU\,\mathbf{r} + rV\,\boldsymbol{\phi})\eta^0 \tag{1.36}$$

$$= \eta_T^0 + \nabla\cdot\mathbf{v}\eta^0 \tag{1.37}$$

where

$$\mathbf{v} \approx (U\,\mathbf{r} + V\,\boldsymbol{\phi}) \tag{1.38}$$

and r_c is the limiting amplitude. Note how U and V (1.23) (1.28) are only functions of the radius, r. We substituted $1/r$ with $1/r_c$ since we are looking at the behavior close to the limit cycle. Thus, in the steady state (no diffusing and $\eta_T^0 = 0$)

$$U(r_c) = V(r_c) = 0 \tag{1.39}$$

To find the phase noise, we need to find the transition probability that a given "dot" will move from one point in phase space to another. This will enable the calculation of the autocorrelation function, which can then be transformed to the power spectral density. In other words, we are looking for the transient response of the phase diffusion given an initial condition in the steady state, which is why we found (1.37) close to the limit cycle (specifically, we are looking for the Green function). To find the phase diffusion PDE in the presence of nonlinearities, U and V, we make another assumption—that the noise is asymptotically smaller than the nonlinearities. This is the strong limit cycle assumption, in which trajectories are

attracted to the limit cycle more than they are diffused by the noise. This is valid in most electronic oscillators since the noise tends to be on the order of Boltzmann's constant, k, which is much smaller than the effects of most nonlinear processes. Thus, to focus on behavior close to the limit cycle, we define a new variable which is centered about r_c and scaled appropriately,

$$x \equiv \frac{r - r_c}{\sqrt{D}} \qquad (1.40)$$

Since diffusion happens on the same scale as the diffusion constant, we scale time as

$$\tau \equiv DT \qquad (1.41)$$

Taking (1.33) and multiplying by r, we get

$$r\eta_T^0 + \left\{rU\eta^0\right\}_r + \eta_\phi^0 V = \frac{1}{2}Dr\eta_{rr}^0 + \frac{1}{2}D\eta_r^0 + \frac{D}{2r}\eta_{\phi\phi}^0 \qquad (1.42)$$

From (1.39), we expand rU and V in powers of $\sqrt{D}x$,

$$rU = -u_1\sqrt{D}x + u_2Dx^2 + u_3D^{3/2}x^3 + \cdots \qquad (1.43)$$

$$V = v_1\sqrt{D}x + v_2Dx^2 + \cdots \qquad (1.44)$$

For the limit cycle to be stable, u_1 has to be positive. Plugging (1.43) and (1.44) into (1.42), we get

$$Dr_c\eta_\tau^0 + \left\{(-u_1x + u_2\sqrt{D}x^2 + u_3Dx^3)\eta^0\right\}_x + \eta_\phi^0(v_1\sqrt{D}x + v_2Dx^2)$$
$$= \frac{1}{2}(r_c + \sqrt{D}x)\eta_{xx}^0 + \frac{1}{2}\sqrt{D}\eta_x^0 + \frac{D}{2r_c}\eta_{\phi\phi}^0$$
$$+ \text{ higher order terms} \qquad (1.45)$$

Collecting terms of the same order,

$$\frac{r_c}{2}\eta_{xx}^0 + \left\{u_1x\eta^0\right\}_x = \sqrt{D}\left(-\frac{x}{2}\eta_{xx}^0 - \frac{1}{2}\eta_x^0 + \left\{u_2x^2\eta^0\right\}_x + \eta_\phi^0 v_1x\right)$$
$$+ D\left(-\frac{1}{2r_c}\eta_{\phi\phi}^0 + r_c\eta_\tau^0 + \left\{u_3x^3\eta^0\right\}_x + \eta_\phi^0 v_2x^2\right)$$
$$+ \text{ higher order terms} \qquad (1.46)$$

11

We now expand η^0 as a perturbation series with $\sqrt{D}$ as the small parameter,

$$\eta^0 = \rho^0 + \sqrt{D}\rho^1 + D\rho^2 + \cdots \tag{1.47}$$

where the superscripts are indices and should not be confused with exponents. We proceed to match orders and derive expressions which can be used to simplify equations until we get to the phase diffusion which occurs at $O(D)$. Starting with the $O(1)$ equation, we find

$$\left\{ \frac{r_c}{2}\rho_x^0 + u_1 x \rho^0 \right\}_x = 0 \tag{1.48}$$

This says that the expression in braces is a constant with respect to x. This constant has to be zero to prevent our solution from blowing up—ρ^0 goes to zero as x tends to positive or negative infinity. Note that despite the fact that x can really only go to $-r_c/\sqrt{D}$, we integrate from negative infinity since all our expressions should tend to zero far away from the limit cycle. Thus,

$$\rho_x^0 = -\frac{2x u_1}{r_c}\rho^0 \tag{1.49}$$

This gives the gaussian solution

$$\rho^0 \sim \exp\left(-\frac{u_1 x^2}{r_c}\right) \tag{1.50}$$

The constant of integration will depend on ϕ and τ. Thus, we write

$$\rho^0(x, \phi, \tau) = \Phi(\phi, \tau)\sqrt{\frac{u_1}{\pi r_c}}\exp\left(-\frac{u_1 x^2}{r_c}\right) \tag{1.51}$$

This shows that the probability distribution about the limit cycle will tend to a gaussian in the strong attraction case. Note how the lack of a time derivative in the $O(1)$ equation implies that the amplitude diffusion occurs at a very fast rate and settles to the prescribed gaussian before the phase even starts diffusing. Moving on

to terms of $O(\sqrt{D})$,

$$\left\{ \frac{r_c}{2}\rho_x^1 + u_1 x \rho^1 \right\}_x = -\frac{x}{2}\rho_{xx}^0 - \frac{1}{2}\rho_x^0 + \left\{ u_2 x^2 \rho^0 \right\}_x + \rho_\phi^0 v_1 x \tag{1.52}$$

$$= \left\{ -\frac{1}{2}x\rho_x^0 + u_2 x^2 \rho^0 \right\}_x + \rho_\phi^0 v_1 x \tag{1.53}$$

Finding the antiderivative of the above expression,

$$u_1 x \rho^1 = -\frac{r_c}{2}\rho_x^1 - \frac{1}{2}x\rho_x^0 + u_2 x^2 \rho^0 - v_1 \Phi_\phi \sqrt{\frac{u_1}{\pi r_c}\frac{r_c}{2u_1}} \exp\left(-\frac{u_1 x^2}{r_c} \right) \tag{1.54}$$

which we then integrate from $x = -\infty$ to $x = \infty$, giving

$$\int_{-\infty}^{\infty} x\rho^1 \, dx = -\frac{1}{2u_1} \int_{-\infty}^{\infty} x\rho_x^0 \, dx + \frac{u_2}{u_1} \int_{-\infty}^{\infty} x^2 \rho^0 \, dx - v_1 \Phi_\phi \frac{r_c}{2u_1{}^2} \tag{1.55}$$

$$= \left(\frac{u_2}{u_1} + \frac{1}{2u_1} \right) \int_{-\infty}^{\infty} x^2 \rho^0 \, dx - \frac{v_1 r_c}{2u_1{}^2}\Phi_\phi \tag{1.56}$$

$$= \frac{u_2 + 1/2}{u_1}\Phi\frac{r_c}{2u_1} - \frac{v_1 r_c}{2u_1{}^2}\Phi_\phi \tag{1.57}$$

$$= \frac{r_c}{2u_1{}^2}\left(\left(u_2 + \frac{1}{2} \right)\Phi - v_1\Phi_\phi \right) \tag{1.58}$$

where we used the regularity condition (ρ^1 goes to zero at the boundaries) to remove one integral in (1.55). We used integration by parts to go from (1.55) to (1.56), and used the fact that ρ^0 was gaussian to calculate the integral in (1.57). We will make use of this integral in the following derivation of the phase diffusion. Now match orders of $O(D)$,

$$\left\{ \frac{r_c}{2}\rho_x^2 + u_1 x \rho^2 \right\}_x = \left\{ -\frac{1}{2}x\rho_x^1 + u_2 x^2 \rho^1 \right\}_x + v_1 x \rho_\phi^1$$
$$- \frac{1}{2r_c}\rho_{\phi\phi}^0 + r_c\rho_\tau^0 + \left\{ u_3 x^3 \rho^0 \right\}_x + \rho_\phi^0 v_2 x^2 \tag{1.59}$$

Integrating x in $(-\infty, \infty)$ and using the regularity conditions,

$$\Phi_\tau + \frac{v_2}{r_c}\partial_\phi \int_{-\infty}^{\infty} x^2 \rho^0 \, dx + \frac{v_1}{r_c}\partial_\phi \int_{-\infty}^{\infty} x\rho^1 \, dx - \frac{1}{2r_c^2}\Phi_{\phi\phi} = 0 \tag{1.60}$$

Now we use (1.58) to get our phase diffusion equation,

$$\Phi_\tau + \left(\frac{v_2}{2u_1} + \frac{v_1}{2u_1^{\,2}}\left(u_2 + \frac{1}{2}\right)\right)\Phi_\phi - \left(\frac{v_1^{\,2}}{2u_1^{\,2}} + \frac{1}{2r_c^2}\right)\Phi_{\phi\phi} = 0 \qquad (1.61)$$

Thus, we see that the nonlinearities contribute to both the advection and diffusion of the phase. Since the coefficients of advection and diffusion in (1.61) depend only on x, we can make substitutions to get our final phase diffusion PDE

$$\Phi_\tau + A\Phi_\phi - B\Phi_{\phi\phi} = 0 \qquad (1.62)$$

with initial condition

$$\Phi(\phi, \tau = 0) = \delta(\phi), \qquad \phi \in (-\pi, \pi] \qquad (1.63)$$

where

$$A = \frac{v_2}{2u_1} + \frac{v_1}{2u_1^{\,2}}\left(u_1 + \frac{1}{2}\right) \qquad (1.64)$$

and

$$B = \frac{v_1^{\,2}}{2u_1^{\,2}} + \frac{1}{2r_c^2} \qquad (1.65)$$

Transforming to a shifted frame where $z \equiv \phi - A\tau$ gives a pure diffusion equation in z and τ. Using this transformation, we find the solution to (1.62)

$$\Phi(\phi, \tau) = \frac{1}{2\pi}\sum_{k=-\infty}^{\infty} e^{-k^2 B|\tau|}e^{ik(\phi - A|\tau|)} \qquad (1.66)$$

which shows how the nonlinearity causes a frequency drift in the oscillator. The nonlinearity (in B) also causes more diffusion. Rewriting (1.66) in terms of the original variables (θ, t),

$$\Phi(\theta, t) = \frac{1}{2\pi}\sum_{k=-\infty}^{\infty} e^{-k^2 BD\epsilon|t|}e^{ik\theta}e^{ik(1 - AD\epsilon)t} \qquad (1.67)$$

where slow time has been converted back to normal time ($\tau = D\epsilon t$) (using (1.41)) and the system rotated back to the non-rotating frame ($\phi = \theta + t$).

Equation (1.67) gives us the phase density of the oscillators in phase space, along with how they flow in time. To find the power spectral density, we need to find the autocorrelation function of v

$$R_{vv}(t) = r_c^2 \langle \sin(\alpha) \sin(\alpha + \beta) \rangle \tag{1.68}$$

$$= r_c^2 \langle \sin^2(\alpha) \cos(\beta) + \sin(\alpha) \cos(\alpha) \sin(\beta) \rangle \tag{1.69}$$

where α is the phase of the "dot" at some time t', and β is the phase difference at a later time, $t' + t$. Over long times (when the oscillator reaches its steady state), α will be uniformly distributed over all angles. We tacitly assume the process is wide-sense stationary, by writing $R_{vv}(t)$ as only a function of the time difference. Consider

$$\Re \left[\langle e^{i\theta} \rangle \right] = \Re \left[e^{-BD\epsilon|t|} e^{-i(1-AD\epsilon)t} \right] = e^{-BD\epsilon|t|} \cos(1 - AD\epsilon)t \tag{1.70}$$

where the expected value can be evaluated by noting that only the $k = -1$ term survives in the sum of (1.67). Thus,

$$R_{vv}(t) = \frac{r_c^2}{2} e^{-BD\epsilon|t|} \cos(1 - AD\epsilon)t \tag{1.71}$$

The Fourier transform of this (see Appendix) is then

$$S_{vv}(\Delta\omega) \approx \frac{\frac{r_c^2}{2} BD\epsilon}{\Delta\omega^2} \tag{1.72}$$

which gives the power spectral density of the phase noise. From the derivation of the diffusion equation, we note that the diffusion constant is proportional to the variance of the Wiener process and its relation given by

$$\epsilon D = \frac{1}{2} S_{ww} \tag{1.73}$$

where S_{ww} is the power spectral density of the $w(t)$ white noise process. Therefore, (1.65), (1.72), and (1.73) give

$$S_{vv}(\Delta\omega) \approx \frac{\left(\frac{v_1{}^2 r_c^2}{8u_1{}^2} + \frac{1}{8} \right) S_{ww}}{\Delta\omega^2} \tag{1.74}$$

15

Note that this is the double-sided power spectral density, if the value plugged in for S_{ww} corresponds to the double-sided density of the noise. Often times, phase noise is also reported as being normalized to the power of the oscillator. Thus, we might also need to find the limiting amplitude.

We can simplify (1.74) if we assume that our nonlinearity, f, depends only on v (voltage in a parallel tank), and not q (current). This is akin to assuming that our nonlinearity is memoryless and one-dimensional. Then, from (1.28), $V = 0$ because f is symmetric about $\theta = \pi/2$ whereas $\cos \theta$ is antisymmetric. Thus, our simplified form for the phase noise is

$$S_{vv}(\Delta \omega) \approx \frac{\frac{1}{8} S_{ww}}{\Delta \omega^2} \tag{1.75}$$

We consider nonconstant diffusion with cyclostationary white noise sources in the appendix. In that case, when $V = 0$ and the attraction to the limit cycle is strong (see Appendix for details), we find

$$S_{vv}(\Delta \omega) \approx \frac{\frac{1}{2\pi} \int_0^{2\pi} \frac{1}{4} S_{ww} \cos^2 \theta \, d\theta}{\Delta \omega^2} \tag{1.76}$$

1.4.2   Limiting amplitude

The limiting amplitude was already found in the previous section. Since we know that U is the velocity in the radial direction (1.38) close to the limit cycle, we can set $U = 0$ in (1.23) to get

$$\int_0^{2\pi} f \sin \theta \, d\theta = 0 \tag{1.77}$$

as a necessary condition for limiting. Thus, finding roots of this integral will give us the possible amplitudes.

However, as a comparison to other perturbation techniques, it is interesting to see how one goes about finding this result with another method, known as the method of averaging. Starting with the same equation (1.2) (1.3), we note that the unperturbed solutions are

$$q = \rho \cos(\phi + t)$$
$$v = -\rho \sin(\phi + t)$$

(1.78)

For the perturbed system, ρ and ϕ will no longer be constants and will have some time dependence. The basic idea behind the method of averaging is to find slow flow equations for these parameters. Thus,

$$\dot{q} = \dot{\rho} \cos(\phi + t) - \rho(\dot{\phi} + 1) \sin(\phi + t)$$
$$\dot{v} = -\dot{\rho} \sin(\phi + t) - \rho(\dot{\phi} + 1) \cos(\phi + t)$$

(1.79)

Inserting the expressions (1.79) into the system (1.3) (without noise) and simplifying,

$$\dot{\rho} = \epsilon f(q, v) \sin(\phi + t)$$
$$\dot{\phi} = -\epsilon \frac{f(q, v)}{\rho} \cos(\phi + t)$$

(1.80)

where (1.78) are the substitutions to be used in $f(q, v)$. At the fixed point, $\dot{\rho} = \dot{\phi} = 0$. Since we only care about the flow of the amplitude ρ, it is acceptable to neglect the phase term. Without loss of generality, we set $\phi = 0$. According to the theory of the method of averaging, because of the factor of ϵ in the flow equations, parameters ρ and ϕ vary slowly, and thus may be held constant over a short period of time, such as one period. Hence, we may also write

$$\dot{\rho} = \frac{\epsilon}{2\pi} \int_0^{2\pi} f(\rho \cos t, -\rho \sin t) \sin t \, dt$$

(1.81)

Thus, the limiting amplitude is found by setting (1.81) equal to 0. The solvability condition for the limiting amplitude, ρ_0, is given by

$$\frac{1}{2\pi} \int_0^{2\pi} f(\rho_0 \cos t, -\rho_0 \sin t) \sin t \, dt = 0$$

(1.82)

1.4.3   Frequency shifts

The presence of nonlinearities in oscillators can also cause the actual frequency of oscillation to shift. We saw this in our derivation of the phase diffusion equation. We found in (1.67) that the deviation in frequency was

$$\omega_{shift} = -AD\epsilon \tag{1.83}$$

From (1.64) and (1.73), we find

$$\omega_{shift} = -\left(\frac{v_2}{4u_1} + \frac{v_1(u_1 + 1/2)}{4u_1^2}\right) S_{ww} \tag{1.84}$$

We see that the diffusion affects the frequency of oscillation. Larger diffusion tends to push the oscillator further from it's nominal frequency. Thus, noisy oscillators not only exhibit large phase noise skirts, but are also placed further from their desired frequency. However, if we make the assumption that our nonlinearities depend only on v (see the tail end of 2.4.1), then $V = 0$ and no frequency shift is present.

1.4.4   Jitter

There are a multitude of definitions for jitter [5], with the appropriate one being the one most suitable to your particular application. We will calculate the variance of the k-period jitter since this appears to be most common. To achieve this, we need to find the distribution of periods of k cycles.

Because we are interested in how particular zero crossings behave, we consider another form of (1.67) which does not wrap around the circle, namely the Gaussian solution of the diffusion equation

$$\eta(\theta, t) = \frac{1}{\sqrt{4\pi\delta\epsilon t}} \exp\left(-\frac{(\theta + t)^2}{4\delta\epsilon t}\right) \tag{1.85}$$

18

where

$$\delta = \frac{D'}{r_c^2} \qquad (1.86)$$

with D' defined in and r_c the limiting amplitude as defined previously. Since the phase of the oscillator decreases with time, the probability that the zero crossing of the kth-cycle will occur for times $T > t$ can be approximated by

$$\Pr\{T > t\} \approx \int_{-2\pi k}^{\infty} \frac{1}{\sqrt{4\pi\delta\epsilon t}} \exp\left(-\frac{(\theta + t)^2}{4\delta\epsilon t}\right) d\theta \qquad (1.87)$$

$$= \frac{1}{\sqrt{\pi}} \int_{\frac{-2\pi k + t}{\sqrt{4\delta\epsilon t}}}^{\infty} e^{-s^2} ds \qquad (1.88)$$

where (1.88) came from making the substitution

$$s = \frac{\theta + t}{\sqrt{4\delta\epsilon t}} \qquad (1.89)$$

The distribution can be found by

$$p(t) = \Pr\{T = t\} = -\frac{d}{dt}\Pr\{T > t\} \qquad (1.90)$$

$$= \frac{1}{\sqrt{\pi}} \exp\left(-\frac{(t - 2\pi k)^2}{4\delta\epsilon t}\right) \frac{d}{dt}\left(\frac{t - 2\pi k}{\sqrt{4\delta\epsilon t}}\right) \qquad (1.91)$$

$$= \frac{1}{\sqrt{4\pi\delta\epsilon t}} \exp\left(-\frac{(t - 2\pi k)^2}{4\delta\epsilon t}\right)\left(\frac{1}{2} + \frac{\pi k}{t}\right) \qquad (1.92)$$

Using (1.92) to find the expected value of the period, we write

$$\mathrm{E}(T) = \int_0^{\infty} \frac{1}{\sqrt{4\pi\delta\epsilon t}} \exp\left(-\frac{(t - 2\pi k)^2}{4\delta\epsilon t}\right)\left(\frac{t}{2} + \pi k\right) dt \qquad (1.93)$$

Asymptotic expressions for the integral (1.93) can be found using Laplace's method (see Appendix), giving

$$\mu = \mathrm{E}(T) \sim 2\pi k \qquad (1.94)$$

as expected. Similarly,

$$\mathrm{E}(T^2) = \int_0^{\infty} \frac{1}{\sqrt{4\pi\delta\epsilon t}} \exp\left(-\frac{(t - 2\pi k)^2}{4\delta\epsilon t}\right)\left(\frac{t^2}{2} + \pi k t\right) dt \sim 4\pi^2 k^2 \qquad (1.95)$$

Note, however, that the variance cannot simply be found by writing

$$\text{Var}(T) = \text{E}(T^2) - \mu^2 = 0 \tag{1.96}$$

and plugging in (1.94) and (1.95) because the leading order terms in both expressions cancel. Thus, to find the variance, higher-order terms must be kept. This is achieved by rewriting the variance as

$$\text{Var}(T) = \text{E}\left((T - \mu)^2\right) \tag{1.97}$$

$$= \int_0^\infty \frac{1}{\sqrt{4\pi\delta\epsilon t}} \exp\left(-\frac{(t - 2\pi k)^2}{4\delta\epsilon t}\right) \left(\frac{1}{2} + \frac{\pi k}{t}\right) (t - 2\pi k)^2 \, dt \tag{1.98}$$

$$\sim 4\pi k\delta\epsilon \tag{1.99}$$

$$= 4\pi k \frac{D'\epsilon}{r_c^2} \tag{1.100}$$

$$= \frac{k}{r_c^2} \int_0^{2\pi} S_{\tilde{w}\tilde{w}} \cos^2\theta \, d\theta \tag{1.101}$$

which shows the increase in variance is proportional to the number of cycles, k. Thus, for oscillators with small jitter, we can relate the expressions for jitter with those of phase noise by assuming that the probability distribution for the k-period jitter is approximately gaussian—(1.92) shows us that this is not always the case. Looking at (1.101) and (1.74),

$$\text{Var}(T) = \frac{8\pi k}{r_c^2} S_{vv}(1) \tag{1.102}$$

1.4.5 Flicker noise

To handle colored noise sources, we need to derive a modified diffusion operator which models the flow of the particular noise. In this work, we assume these non-white processes to be Markov and gaussian. Because of the gaussianity, calculating the mean-square distance, or variance, is sufficient to describe the process. Although

this may seem restrictive at first, these assumptions are valid if we assume the charge-trapping model of flicker noise.

To find the modified diffusion operator, we note that the mean-square distance, $\langle d^2 \rangle$, of a random path which is assumed to have gaussian increments appears in the solution for the probability density as

$$\eta(\phi, T) \sim \sum_k C(\phi)\, e^{-k^2 \langle d^2 \rangle} \tag{1.103}$$

just as in the white noise case (1.67). Note that $\langle d^2 \rangle$ is dependent on time, t, and is equal to $2Dt$ for a white noise process with diffusion constant D. The density (1.103) is only valid for small $\langle d^2 \rangle$ over the interval $\phi \in (-\pi, \pi]$. This is because large variances lead to wrapping around the $(-\pi, \pi]$ interval, which makes (1.103) not look like a gaussian curve. Small variances, on the other hand, lead to (1.103) being very small near the edges of the interval, and thus looking more like a gaussian that extends to infinity.

Now looking at (1.103), we see that it is the solution of the modified diffusion equation,

$$\eta_T = \partial_T \left\langle d^2 \right\rangle \eta_{\phi\phi} \tag{1.104}$$

This is easy to show using separation of variables on (1.104). Following a derivation similar to the one used to derive the phase diffusion equation (1.62), we find

$$\Phi_T \sim \frac{\Phi_{\phi\phi}}{2\pi r_c^2} \int_0^{2\pi} \frac{1}{2} \partial_T \left\langle d^2 \right\rangle \cos^2 \theta \, d\theta \tag{1.105}$$

The solution to (1.105) is

$$\Phi(\theta, t) = \frac{1}{2\pi} \sum_{k=-\infty}^{\infty} e^{-\frac{\epsilon}{r_c^2} k^2 \int D'\, dt}\, e^{ik\theta} e^{ikt} \tag{1.106}$$

where

$$D' = \frac{1}{2\pi} \int_0^{2\pi} \frac{1}{2} \partial_T \left\langle d^2 \right\rangle \cos^2 \theta \, d\theta \tag{1.107}$$

Thus, in a fashion similar to the way we found (1.71), we get

$$R_{vv}(t) = \frac{r_c^2}{2} e^{-\frac{\epsilon}{r_c^2} \int D' \, dt} \cos t \tag{1.108}$$

This time, however, D' is a function of t, and thus the Fourier transform is no longer a simple Lorentzian. Plugging in (1.107) into (1.108),

$$R_{vv}(t) = \frac{r_c^2}{2} e^{-\frac{1}{r_c^2} \frac{1}{2\pi} \int_0^{2\pi} \frac{1}{2} \langle d^2 \rangle \cos^2 \theta \, d\theta} \cos t \tag{1.109}$$

We now find $\langle d^2 \rangle$.

As in the derivation of the diffusion equation, we now find the variance of the random walk. The total distance walked at time t' is

$$d = \int_0^{t'} X(s) \, ds \tag{1.110}$$

where $X(s) \, ds$ is the incremental distance. Therefore,

$$d^2 = \int_0^{t'} \int_0^{t'} X(s) X(t) \, ds \, dt \tag{1.111}$$

To get the mean-square distance, we take the expectation

$$\langle d^2 \rangle = \int_0^{t'} \int_0^{t'} \mathrm{E}\left(X(s) X(t)\right) \, ds \, dt = \int_0^{t'} \int_0^{t'} R(s, t) \, ds \, dt \tag{1.112}$$

Now it is instructive at this point to look at how the autocorrelation function can be viewed in this two-time space. If we try to plot the autocorrelation function with finite correlation time in the s-t plane, we might see something like Fig. 1.2. The darkness of color represents the correlation, with black being very correlated and white being close to no correlation. This is centered about the line $t = s$, because the
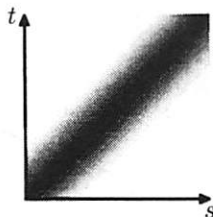

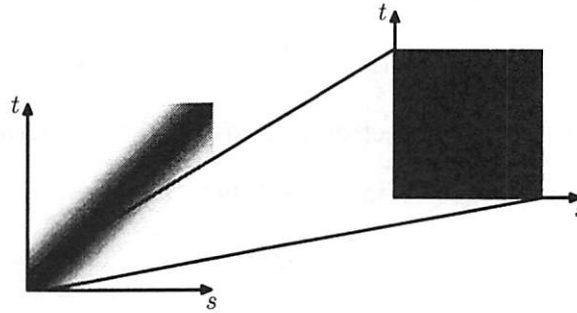Figure 1.2   2-dimensional plot of autocorrelation function.

22

Figure 1.3   Short elapsed time leads to full correlation.

same point is obviously correlated to itself. The area integral, from (1.112), is thus simply the mean-square distance, $\langle d^2 \rangle$.

From this, two limiting cases can be seen. If we first assume small elapsed time, t', we get Fig. 1.3, which is a very zoomed-in picture of Fig. 1.2. Here, the path is very highly correlated, and in the limiting case as t' is small enough, is fully correlated. The mean-square distance, $\langle d^2 \rangle$ is this case is just a constant multiplied by t'^2, hence

$$\langle d^2 \rangle \sim t'^2 \tag{1.113}$$

in this case. In the other extreme, we can take very long elapsed times and look at a zoomed-out plot as in Fig. 1.4. Here, the path looks like a path with no correlation, which would simply be the white noise case. The area integral would now be
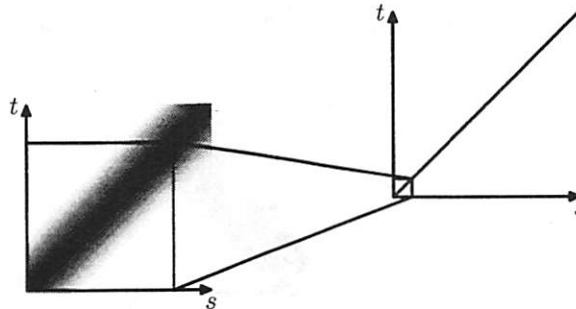

Figure 1.4   Long elapsed time leads to no correlation.

proportional to t',

$$\langle d^2 \rangle \sim t' \tag{1.114}$$

The mean-square distance of colored noise with finite correlation times would then be somewhere in between (1.113) and (1.114).

Now going back to the flicker noise problem, we use the autocorrelation function of the charge-trapping model of flicker noise to find the mean-square distance traveled at time, t'. We first assume the autocorrelation function is wide-sense stationary and equal to

$$R(s,t) = e^{-\lambda |s-t|} \tag{1.115}$$

where $\tau = 1/\lambda$ is the time constant dependent on how long charges are stored in interface traps. Actually, this autocorrelation function corresponds to random telegraph noise which has a Lorentzian distribution. A superposition of many of these processes with varying time constants will result in a process with a $1/f$ distribution. The superposition is valid since we assume the different traps behave independently. For now, we will focus on (1.115) as integrating over the time constant will pose no difficulty. Finding the mean-square path, we get

$$\langle d^2 \rangle (t') = \int_0^{t'} \int_0^{t'} e^{-\lambda |s-t|} \, ds \, dt \tag{1.116}$$

$$= \int_0^{t'} \left(\int_0^t e^{-\lambda(t-s)} \, ds + \int_t^{t'} e^{-\lambda(s-t)} \, ds \right) dt \tag{1.117}$$

$$= \int_0^{t'} \left(\frac{1}{\lambda} - \frac{1}{\lambda} e^{-\lambda t} + \frac{1}{\lambda} - \frac{1}{\lambda} e^{-\lambda(t'-t)} \right) dt \tag{1.118}$$

$$= \frac{2}{\lambda} t' + \frac{2}{\lambda^2} \left(e^{-\lambda t'} - 1 \right) \tag{1.119}$$

$$= \frac{2}{\lambda} \left(t' + \frac{1}{\lambda} \left(e^{-\lambda t'} - 1 \right) \right) \tag{1.120}$$

Thus, if $\tau = \frac{1}{\lambda}$ is $O(\epsilon)$, we see that the mean-square distance is small. We will make

this assumption. Note that

$$\langle d^2 \rangle \to \lambda t'^2, \qquad t' \to 0 \tag{1.121}$$

$$\langle d^2 \rangle \to \frac{2}{\lambda} t', \qquad t' \to \infty \tag{1.122}$$

which agrees with (1.113) and (1.114). To find the modified diffusion operator, we find

$$\partial_T \langle d^2 \rangle = \frac{1}{\epsilon} \partial_t \langle d^2 \rangle (t) \tag{1.123}$$

$$= \frac{2}{\epsilon \lambda} \left(1 - e^{-\lambda t} \right) \tag{1.124}$$

We see that the diffusion operator is $O(1)$. Now substituting (1.120) into (1.109), we get

$$R_{vv}(t) = \frac{r_c^2}{2} e^{-\frac{1}{r_c^2} \frac{1}{2\pi} \int_0^{2\pi} \frac{1}{2} \langle d^2 \rangle \cos^2 \theta \, d\theta} \cos t \tag{1.125}$$

Finding the Fourier transform of this to get the power spectral density (see Appendix), we arrive at

$$S_{vv}(\omega) = \frac{1}{\Delta\omega^2} \frac{\lambda/4}{\lambda^2 + \Delta\omega^2} \tag{1.126}$$

This, however, is the noise spectral density due to a *single* interface trap. In order to model flicker noise, we need to find the distribution of traps in the interface and average over them. As mentioned in [4], the time constant for an interface trap is exponentially related to the distance from the surface,

$$\tau = \tau_0 \exp(\gamma z) \tag{1.127}$$

$$\tau_1 = \tau_0 \exp(\gamma z_1) \tag{1.128}$$

where the tunneling parameter, γ, depends on properties of the material (oxide) in which the traps are buried. Thus, assuming a uniform trap distribution between

$0 < z < z_1$, we find the distribution for τ,

$$d\tau = \tau\gamma\,dz \qquad\qquad (1.129)$$

$$= \tau\frac{\ln(\tau_1/\tau_0)}{z_1}\,dz \qquad\qquad (1.130)$$

Thus,

$$\frac{dz}{z_1} = \frac{1/\tau\,d\tau}{\ln(\tau_1/\tau_0)} \qquad\qquad (1.131)$$

The autocorrelation function (1.115) for the single trap, when averaged over all time constants (1.131) gives the $1/f$ distribution mentioned earlier,

$$\mathcal{F}\left[\int_0^{z_1} e^{-\lambda|t|}\frac{1}{z_1}\,dz\right] = \int_0^{z_1}\int_{-\infty}^{\infty} e^{-\lambda|t|}e^{-i\omega t}\,dt\frac{1}{z_1}\,dz \qquad\qquad (1.132)$$

$$= \int_0^{z_1} \frac{2\lambda}{\lambda^2+\omega^2}\frac{1}{z_1}\,dz \qquad\qquad (1.133)$$

$$= \frac{2}{\ln(\tau_1/\tau_0)}\int_{\tau_0}^{\tau_1} \frac{1}{1+\omega^2\tau^2}\,d\tau \qquad\qquad (1.134)$$

$$= \frac{2}{\omega\ln(\tau_1/\tau_0)}\left(\tan^{-1}(\omega\tau_1) - \tan^{-1}(\omega\tau_0)\right) \qquad\qquad (1.135)$$

The power spectral density, (1.135), has a $1/f$ slope between two edges where the
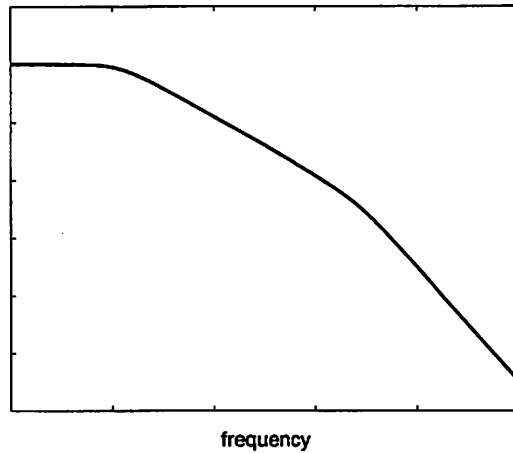

frequency

Figure 1.5 Sample plot of power spectral density (1.135).

density either flattens out or steepens to $1/f^2$ Fig. 1.5. Using

$$\tan^{-1}(x) \approx x - \frac{x^3}{3} + O(x^5) \tag{1.136}$$

for x small, and

$$\tan^{-1}(x) \approx \frac{\pi}{2} \tag{1.137}$$

for x large, we find that the power spectral density in the "$1/f$" ($1/\tau_1 \ll \omega \ll 1/\tau_0$) region,

$$S(\omega) \approx \frac{\pi}{\omega \ln(\tau_1/\tau_0)} \tag{1.138}$$

Now looking back at (1.126), the expression for the noise spectral density of flicker noise in oscillators is

$$S_{vv}(\Delta\omega) = \int_0^{z_1} \frac{1}{\Delta\omega^2} \frac{\lambda/4}{\lambda^2 + \Delta\omega^2} \frac{1}{z_1} \, dz \tag{1.139}$$

$$\approx \frac{1}{\Delta\omega^3} \frac{\pi/8}{\ln(\tau_1/\tau_0)} \tag{1.140}$$

$$= \frac{S(1)/8}{\Delta\omega^3} \tag{1.141}$$

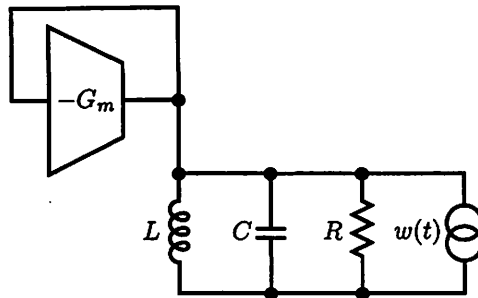## 1.5   Simplified models: Van der Pol oscillator

Figure 1.6   Simplified feedback oscillator.

A simplified model of a feedback oscillator, often used to illustrate the basic mechanisms of an electronic oscillator, is shown in Fig. 1.6. The finite Q of the parallel LC
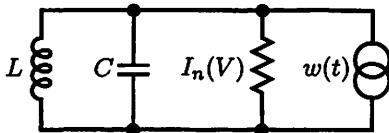
Figure 1.7   Van der Pol oscillator.

tank is modeled by a parallel resistor. The basic regenerative element is the feedback transconductor. The noise that it generates is modeled by a shunt current source. In the steady-state, this regenerative element may be approximated by a linear transconductor. However, to model amplitude limiting, the transconductor would need to be nonlinear. For this part

of the problem, we assume a basic polynomial nonlinearity. This specific nonlinearity was first derived by Van der Pol for vacuum-tube oscillators. Although it may not be as completely applicable to modern transistor oscillators, it is often used as a simple example to illustrate features of nonlinear oscillators. The circuit diagram for the Van der Pol oscillator is shown in Fig. 1.7. The differential equation describing this oscillator is

$$C\frac{dV}{dt} + \frac{1}{L}\int V\,dt + I_n(V) = \bar{w}(t) \tag{1.142}$$

where

$$I_n(V) = -\frac{1}{R}\left(V - \frac{1}{3}a_1 V^3\right) \tag{1.143}$$

is the current flowing through the nonlinear resistance. In order for the oscillator to have a limiting amplitude, a_1 needs to be a positive constant. Rewriting (1.142) with the substitution

$$q = \int V\,dt \tag{1.144}$$

gives

$$\ddot{q} + \frac{1}{LC}q - \frac{1}{RC}\left(1 - \frac{1}{3}a_1\dot{q}^2\right)\dot{q} = \frac{1}{C}\bar{w}(t) \tag{1.145}$$

Nondimensionalizing (1.145) with,

$$\frac{t}{\sqrt{LC}} \to t \qquad \frac{q}{\sqrt{\frac{3}{a_1}\sqrt{LC}}} \to q \tag{1.146}$$

gives

$$\ddot{q} + q = \epsilon\left(1 - \dot{q}^2\right)\dot{q} + w(t) \tag{1.147}$$

where

$$\epsilon = \frac{\sqrt{LC}}{RC} \qquad w(t) = \frac{\bar{w}(t)}{\sqrt{\frac{3}{a_1}}\sqrt{\frac{C}{L}}} \tag{1.148}$$

Note that the small parameter $\epsilon = 1/Q$, which means that the systems we will focus on are high-Q oscillators, or systems which have near sinusoidal oscillations. The limit cycle in these systems will be near circular since they are close to the linear harmonic oscillator. Referring to (1.2), the nonlinearity is

$$f(q,v) = (1 - v^2)v \tag{1.149}$$

Plugging (1.149) into (1.82), the limiting amplitude is found through the relation

$$-\frac{1}{2\pi}\int_0^{2\pi}\left(1 - \rho_0^2\sin^2 t\right)\rho_0\sin^2 t\, dt = 0 \tag{1.150}$$

Solving for ρ_0,

$$\frac{1}{2}\rho_0 - \frac{3}{8}\rho_0^3 = 0 \tag{1.151}$$

and throwing away the trivial solution $\rho_0 = 0$, reveals that

$$\rho_0 = \frac{2}{\sqrt{3}} \tag{1.152}$$

Putting the units back in for $v = \dot{q}$, we get

$$\rho_0 = \frac{2}{\sqrt{a_1}} \tag{1.153}$$

Assuming the noise source is stationary (time-invariant) white noise with single-sided power spectral density of $4kT/R$, (1.75) gives the normalized output voltage noise as

$$S_{vv}(\omega) = \frac{a_1}{6} kT \frac{L}{RC} \frac{1}{\Delta\omega^2} \tag{1.154}$$

where (1.148) was used to nondimensionalize the noise. Now note that if $F(\omega)$ is the Fourier transform of a function $f(t)$ in terms of unitless time, t, then the Fourier transform of $f(t/t_s)$, the same function written in terms of dimensioned time, is $t_s F(\omega t_s)$. Thus, putting the units back into (1.154),

$$S_{vv}(\omega) = \frac{1}{2} \frac{kT}{RC^2} \frac{1}{\Delta\omega^2} \tag{1.155}$$

using (1.146) and noting that the dimensions of the power spectral density is in $v^2 t$. Since the units of $1/\Delta\omega^2$ is t^2, which we accounted for when we rescaled time in finding the Fourier transform, we multiply by

$$\frac{3}{a_1 \sqrt{LC}} \tag{1.156}$$

which has units v^2/t to adjust for the overall units. Note that these are precisely the units of the diffusion constant, as it appears in the numerator of (1.75).

Finding the phase noise as the ratio of the output voltage noise power to the power of the carrier,

$$\mathcal{L}(\omega) = \frac{1}{\rho_0^2} \frac{kT}{RC^2} \frac{1}{\Delta\omega^2} \tag{1.157}$$

$$= \frac{a_1}{4} \frac{kT}{RC^2} \frac{1}{\Delta\omega^2} \tag{1.158}$$

$$= \frac{a_1}{4} \frac{kT}{QC} \frac{\omega_0}{\Delta\omega^2} \tag{1.159}$$

where we used $Q = \omega_0 RC$ and $\omega_0 = 1/\sqrt{LC}$. Thus, we see from (1.159) that, for a given oscillation frequency, ω_0, and a fixed Q (assuming the tank Q is determined
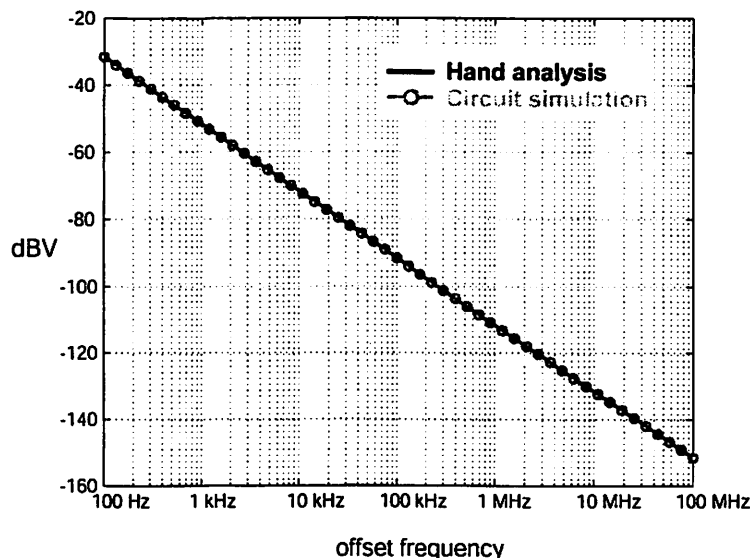
Figure 1.8   Comparison between hand-analytical equation and SpectreRF simulations for a Van der Pol oscillator with injected stationary white noise.

largely by the inductor), phase noise decreases with increasing capacitance. Note that the limiting amplitude in this Van der Pol oscillator is independent of the component values and depends only on the nonlinearity, a_1. This need not be the case in other oscillator topologies.

Using sample values for the components, $L = 50\,\text{pH}$, $C = 141\,\text{fF}$, $R = 377\,\Omega$ (corresponds to a Q of 20), $a_1 = 3$, and injecting a current noise equal to $4kT/R$ for the resistor, we see good matching between simulations using the SpectreRF circuit simulator and our equation (1.155) for the output voltage noise (Fig. 1.8). The equation for the limiting amplitude (1.153), calculated to be $\rho_0 = 1.155$, also shows close matching to simulations (Fig. 1.9).

Considering non-stationary white noise, such as cyclostationary noise which depends on the instantaneous tank voltage, we start from (1.76). This time, our white noise spectral density is not constant. Modeling the cyclostationary noise current in our Van der Pol oscillator as being proportional to the instantaneous resistance, we

31
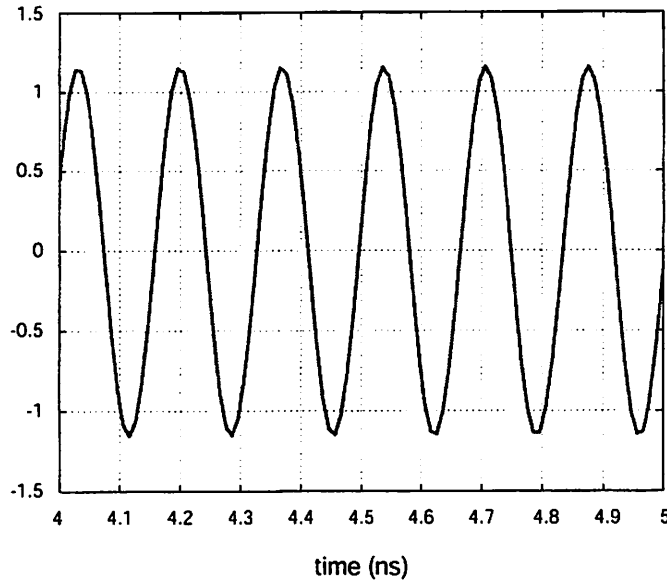
Figure 1.9 Steady-state waveform of the Van der Pol oscillator with $a_1 = 3$.

use

$$S_{\tilde{w}\tilde{w}} = 4kT\frac{1}{R}\left|1 - 3v^2\right| \tag{1.160}$$

in (1.74) to get

$$S_{vv}(\Delta\omega) = \frac{1}{\Delta\omega^2}\frac{1}{2\pi}\int_0^{2\pi}\frac{kT}{R}\left|1 - 3v^2\right|\cos^2\theta\,d\theta \tag{1.161}$$

$$= \frac{1}{\Delta\omega^2}\frac{1}{2\pi}\int_0^{2\pi}\frac{kT}{R}\left|1 - 3\rho_0^2\sin^2\theta\right|\cos^2\theta\,d\theta \tag{1.162}$$

The use of absolute value signs is necessary since noise never helps and adds to diffusion, regardless of whether the instantaneous resistance is negative (growing oscillation) or positive (decaying oscillation). Note that (1.162) is again in dimensionless variables, so $\rho_0 = 2/\sqrt{3}$. This expression can be numerically integrated to give

$$S_{vv}(\Delta\omega) = \frac{0.413496\,\dfrac{kT}{RC^2}}{\Delta\omega^2} \tag{1.163}$$
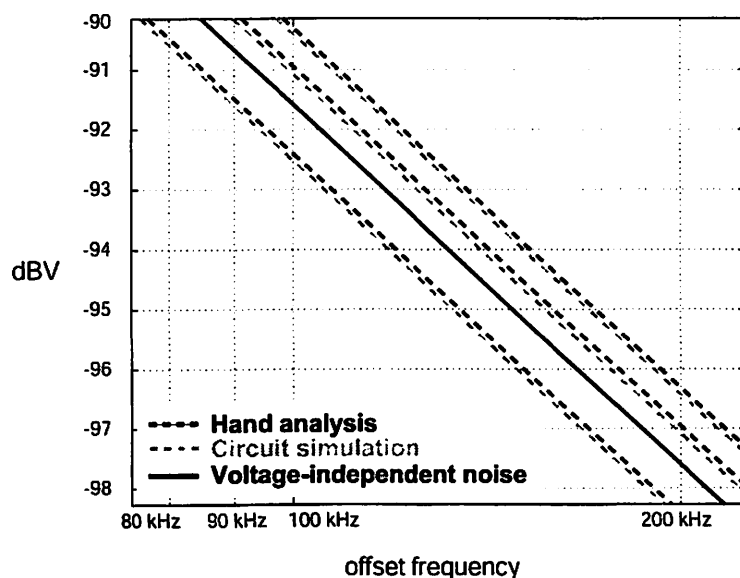
Figure 1.10   Comparison between hand-analytical equations and SpectreRF simulation for modified Van der Pol-like oscillators with cyclostationary white noise.

Comparisons between (1.163) and SpectreRF simulations are shown in Fig. 1.10. In addition to the time-varying noise due to a cubic nonlinearity (1.163), similar expressions for 5th and 7th order polynomial nonlinearities were also derived and compared against SpectreRF.

1.6   Pierce oscillator
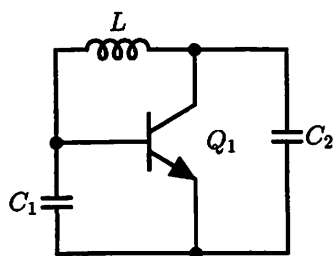
Figure 1.11   Pierce oscillator.

The simplified circuit schematic for the Pierce oscillator is shown in Fig. 1.11. We model the finite Q of the inductor with a parallel resistance, R. The simplified

differential equation governing this circuit is then

$$I_L + I_R = I(V_o, V_b) + C_2 \frac{d}{dt} V_o - \bar{w}(t) \tag{1.164}$$

where the transistor current, $I(V_o, V_b)$, is nonlinear and looks exponential. The noise injected into the node V_o due to the transistor and the resistor is modeled as a current source with magnitude $\bar{w}(t)$. The white noise source, $\bar{w}(t)$, in this circuit is a zero-mean cyclostationary source.

If we make the approximation that the capacitive transformer formed by C_2 and C_1 is nearly ideal, in that the bulk of the high-frequency current does not flow through the emitter, we can write

$$V_b \approx -kV_o \tag{1.165}$$

where

$$k = \frac{C_2}{C_1} \tag{1.166}$$

This, of course, assumes that power is getting into the circuit somehow. Not pictured in the simplified schematic is a bias resistor which feeds the supply power into the collector of the transistor. This resistor behaves like a choke and can be safely neglected in our calculations. Expanding the differential equation (1.164) in terms of circuit components,

$$-\frac{1}{L} \int (1 + k) V_o \, dt - (1 + k)\frac{V_o}{R} = I(V_o) + C_2 \frac{d}{dt} V_o - \bar{w}(t) \tag{1.167}$$

Defining

$$q = \int V_o \, dt \tag{1.168}$$

we get

$$\ddot{q} + \frac{1}{LC_T} q = -\frac{1}{RC_T} \dot{q} - \frac{1}{C_2} I(\dot{q}) + \frac{1}{C_2} \bar{w}(t) \tag{1.169}$$

where we defined

$$C_T = \frac{C_1 C_2}{C_1 + C_2} \tag{1.170}$$

$$= \frac{C_2}{1 + k} \tag{1.171}$$

Nondimensionalizing time with

$$\frac{t}{\sqrt{LC_T}} \to t \tag{1.172}$$

we find

$$\ddot{q} + q = -\frac{\sqrt{LC_T}}{RC_T}\dot{q} - \frac{LC_T}{C_2}I(\dot{q}) + \frac{LC_T}{C_2}\bar{w}(t) \tag{1.173}$$

Choosing our small parameter ϵ to be

$$\epsilon = \frac{\sqrt{LC_T}}{RC_T} \tag{1.174}$$

we find our nonlinearity, f in (1.2), to be

$$f(\dot{q}) = -\dot{q} - \frac{\sqrt{LC_T}R}{1 + k}I(\dot{q}) \tag{1.175}$$

$$= -\dot{q} - \frac{\sqrt{LC_T}R}{1 + k}\left(I_s \exp\left(\frac{V_s - k\dot{q}}{V_T}\right)\right) \tag{1.176}$$

Since the shot noise in a BJT is simply

$$S_{\bar{w}\bar{w}} = 2q'I \tag{1.177}$$

where q' is the electronic charge, we can write our diffusion as a function of f. Thus, finding the phase noise from (1.76),

$$S_{vv}(\Delta\omega) \approx \frac{\frac{1}{2\pi}\int_0^{2\pi}\frac{1}{2}q'I(\dot{q})\cos^2\theta\,d\theta}{\sqrt{LC_T}\Delta\omega^2} \tag{1.178}$$
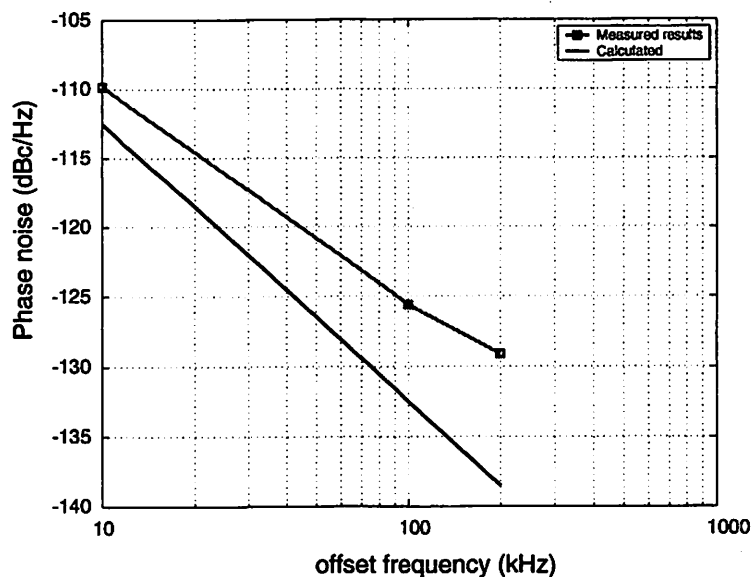
Figure 1.12   Comparison between calculated values for phase noise and measured results.

Fig. 1.12 shows a plot of (1.178) against measured phase noise from a BJT Pierce oscillator operating at 12 MHz. Due to somewhat inaccurate measurements, both plots do not necessarily agree. More importantly, what was learned from this exercise is that by viewing the generation of phase noise as a diffusion process, we see that by making our attraction to the limit cycle stronger, we reel in the trajectories and cause them to diffuse less. Since the velocities in the phase direction are greater when off the limit cycle (since we showed that it is zero in the rotating frame on the limit cycle), weaker attraction of any kind will result in larger diffusing. In generating our results for Fig. 1.12, we used a δ-function as an approximation for the distribution of the amplitude spread. As mentioned above, this underpredicts the phase noise and thus could be a reason for the lack of solid agreement between the two graphs.

Also, from (1.178), we see that there are certain values of θ, (when $\cos^2 \theta=0$) which correspond to points where the white noise source does not contribute to phase noise. These points correspond to the nulls in the voltage oscillation. Thus, by designing

36

oscillators which minimize diffusion when at nulls, we minimize our resulting phase noise. In the BJT Pierce oscillator shown, this corresponds to minimizing injected current because the shot noise in a BJT is proportional to the current. For a MOS-FET, on the other hand, since the diffusion is proportional to the transconductance, g_m, we would want to minimize the derivative of the current.

Another way to reduce phase noise would be to decrease the amount of diffusion. Besides the obvious decision to reduce overall noise, we see that diffusion is also largely affected by the capacitances in circuits with parallel LC tanks. Increasing capacitance would decrease diffusion. Intuitively, we may think of this as making our circuit more sluggish, hence more resistant to random perturbations.

APPENDIX

A.1.1   ADVECTION

Let the flow map be described by

$$\dot{\mathbf{x}}(t) = \mathbf{u}(\mathbf{x}(t), t) \tag{1.179}$$

By following a given region $R(t)$, we can write expressions for the advection of the material. Invoking conservation of mass, we get

$$\frac{d}{dt} \int_{R(t)} c(\mathbf{x}, t) \, d\mathbf{x} = 0 \tag{1.180}$$

where $c(\mathbf{x}, t)$ is the concentration at $\mathbf{x}$ at time t. By Leibniz's rule, we can write

$$\frac{d}{dt} \int_R c \, d\mathbf{x} = \int_R c_t \, d\mathbf{x} + \int_{\partial R} cv \, da \tag{1.181}$$

where $\mathbf{v}$ is the velocity vector parallel to the deformation of the region. We know that

$$\mathbf{v} = \mathbf{u} \cdot \mathbf{n} \tag{1.182}$$

where n is the unit normal vector and da is the differential area element. Thus,

$$\frac{d}{dt}\int_R c\,d\mathbf{x} = \int_R c_t\,d\mathbf{x} + \int_R \nabla\cdot(c\mathbf{u})\,d\mathbf{x} = 0 \qquad (1.183)$$

where we have applied the divergence rule. Since this must be true for any region $R(t)$ that we decide to follow, we get

$$\int_R c_t + \nabla\cdot(c\mathbf{u})\,d\mathbf{x} = 0 \quad\Longrightarrow\quad c_t + \nabla\cdot(c\mathbf{u}) = 0 \qquad (1.184)$$

which is the advection equation.

A.1.2 DIFFUSION

Let l_i be the increments due to uncorrelated noise, and let d be the total distance traveled by these increments (a random walk). Then

$$d = \sum_i l_i \qquad (1.185)$$

and the squared length is

$$d^2 = d\cdot d = \sum_{j,k} l_j\cdot l_k \qquad (1.186)$$

where the dot notation would be used in higher dimensional noise increments. Averaging the square distance, we get

$$\langle d\cdot d\rangle = \sum_{j,k}\langle l_j\cdot l_k\rangle \qquad (1.187)$$

Since the noise is uncorrelated between increments, $\langle l_j\cdot l_k\rangle = 0$ for $j\neq k$ and $\langle l_j\cdot l_k\rangle = l^2$ for $j = k$. Thus,

$$\langle d\cdot d\rangle = Nl^2 \qquad (1.188)$$

where N is the number of steps taken. If we assume each step takes time τ, we get $N = \frac{t}{\tau}$ and

$$\langle d\cdot d\rangle = \frac{l^2 t}{\tau} \qquad (1.189)$$

We denote this by

$$\langle d \cdot d \rangle = 2Dt \tag{1.190}$$

where the diffusion coefficient is defined by

$$D = \frac{1}{2}\frac{l^2}{\tau} \tag{1.191}$$

Now call $\rho(x, t)$ the distribution of particles that move a distance x in an elapsed time t. This is equivalent to the transition probability. Then, integrating over all space,

$$\int \rho \, dl = 1 \tag{1.192}$$

Since the noise increments are symmetric in all directions, we also get

$$\int l_i\rho \, dl = 0 \tag{1.193}$$

and

$$\int l_j l_k \rho \, dl = 0, \quad j \neq k \tag{1.194}$$

This is just the averaging in integral form (evaluating the brackets). Now let $c(x, t)$ be the concentration of a state at a position x and time t. In probability terms, this would be the probability of being at x at time t, which differs from the transition probability. We can then write the Chapman-Kolmogorov equation as

$$c(x, t + s) = \int c(y, t)\rho(x - y, s) \, dy \tag{1.195}$$

Changing variables, we write this as

$$c(x, t + s) = \int c(x - z, t)\rho(z, s) \, dz \tag{1.196}$$

We then Taylor expand $c(x, t)$ on both sides of the equation and match orders, getting

$$c(x, t) + sc_t(x, t) + \cdots = \int c(x, t)\rho(z, s) \, dz - \int zc_x(x, t)\rho(z, s) \, dz$$
$$+ \frac{1}{2}\int z^2 c_{xx}(x, t)\rho(z, s) \, dz + \cdots \tag{1.197}$$

$$= c(x, t) - \langle z \rangle c_x(x, t) + \frac{1}{2}\langle z^2 \rangle c_{xx}(x, t) + \cdots \tag{1.198}$$

$$= c(x, t) + sDc_{xx}(x, t) + \cdots \tag{1.199}$$

Therefore, as $s \to 0$, we get

$$c_t = Dc_{xx} = D\Delta c \tag{1.200}$$

which is exactly the diffusion equation.

A.1.3 NONCONSTANT DIFFUSION

To handle cyclostationary white noise sources, we need to allow the diffusion constant, D in (1.4), to depend on the state. For most electronic devices, D depends only on the voltage, v. Not making this assumption makes the problem hard. Our Fokker-Planck equation (1.4) is then

$$\eta_t + \nabla \cdot ((v\,1 - q\,2)\eta + \epsilon f(q,v)\eta\,2) - \epsilon \partial_v D(v)\eta_v = 0 \tag{1.201}$$

The derivation follows the same reasoning and perturbation expansion. Equation (1.17), however, will be replaced by

$$K = -\int_0^{2\pi} \left(\sin(\phi - t)\partial_r - \frac{1}{r}\cos(\phi - t)\partial_\phi \right) D(r,\phi)$$
$$\left(\sin(\phi - t)\partial_r - \frac{1}{r}\cos(\phi - t)\partial_\phi \right) \eta^0 \, dt \tag{1.202}$$

where the diffusion constant was moved into the integral. The evaluation of (1.202) leads to

$$-K = \int_0^{2\pi} \frac{2D}{r} \sin\theta\cos\theta\,\eta_{\phi r}^0 \, dt - \int_0^{2\pi} \frac{2D}{r^2} \sin\theta\cos\theta\,\eta_\phi^0 \, dt$$
$$+ \int_0^{2\pi} \frac{D_\phi}{r} \sin\theta\cos\theta\,\eta_r^0 \, dt + \int_0^{2\pi} \frac{D_r}{r} \sin\theta\cos\theta\,\eta_\phi^0 \, dt$$
$$+ \int_0^{2\pi} \frac{D_\phi}{r^2} \cos^2\theta\,\eta_\phi^0 \, dt + \int_0^{2\pi} D_r \sin^2\theta\,\eta_r^0 \, dt$$
$$+ 2\pi D'' \eta_{rr}^0 + 2\pi \frac{D'}{r}\eta_r^0 + 2\pi \frac{D'}{r^2}\eta_{\phi\phi}^0 \tag{1.203}$$

where

$$D' = \frac{1}{2\pi} \int_0^{2\pi} D \cos^2 \theta \, d\theta \qquad (1.204)$$

$$D'' = \frac{1}{2\pi} \int_0^{2\pi} D \sin^2 \theta \, d\theta \qquad (1.205)$$

We see that for D constant, $D' = D'' = D/2$. Note that for shorthand purposes, $\theta = \phi - t$ in all these integrals.

Going back to our original problem, since D depends only on v, $D(v) = D(r \sin \theta)$ is symmetric about $\theta = \pi/2$. Then, $D \sin \theta$ will also be even about $\theta = \pi/2$. This means that $D \sin \theta \cos \theta$ is an odd function about $\theta = \pi/2$. The integrals containing $D \sin \theta \cos \theta$ thus evaluate to 0! Using the same reasoning, the integral containing $D_r \sin \theta \cos \theta$ also goes to 0 since differentiating with respect to r does not change the parity with respect to $\theta = \pi/2$. Now note that D_ϕ, on the other hand, is going to be odd (derivatives of even functions are odd). Thus, we simplify (1.203) to

$$-K = \int_0^{2\pi} \frac{D_\phi}{r} \sin \theta \cos \theta \, \eta_r^0 \, dt + \int_0^{2\pi} D_r \sin^2 \theta \, \eta_r^0 \, dt$$
$$+ 2\pi D'' \eta_{rr}^0 + 2\pi \frac{D'}{r} \eta_r^0 + 2\pi \frac{D'}{r^2} \eta_{\phi\phi}^0 \qquad (1.206)$$

Now integrating the first integral on the right-hand side by parts, we get

$$\frac{\eta_r^0}{r} \int_0^{2\pi} D_\phi \sin \theta \cos \theta \, dt = 2\pi (D'' - D') \frac{\eta_r^0}{r} \qquad (1.207)$$

and so, we write

$$-\frac{K}{2\pi} = D'' \eta_{rr}^0 + \frac{D''}{r} \eta_r^0 + \frac{D'}{r^2} \eta_{\phi\phi}^0 + D_r'' \eta_r^0 \qquad (1.208)$$

We try to further simplify by defining two constants (may depend on r),

$$D_0 = \frac{1}{2\pi} \int_0^{2\pi} D \, d\theta \qquad (1.209)$$

$$D_2 = \frac{1}{2\pi} \int_0^{2\pi} D \cos 2\theta \, d\theta \qquad (1.210)$$

41

D_0 is the average of the diffusion constant over the period, and D_2 is like the Fourier coefficient of the double frequency. Expanding $\cos^2 \theta$ and $\sin^2 \theta$ using the double-angle formulas, we get

$$D' = \frac{D_0}{2} + \frac{D_2}{2} \tag{1.211}$$

$$D'' = \frac{D_0}{2} - \frac{D_2}{2} \tag{1.212}$$

Thus, we get our final expression for (1.17)

$$-\frac{K}{2\pi} = \frac{D_0}{2}\Delta\eta^0 - \frac{D_2}{2}\Delta\eta^0 + \frac{D_2}{r^2}\eta^0_{\phi\phi} + \frac{(D_{0r} - D_{2r})}{2}\eta^0_r \tag{1.213}$$

Note how the diffusion terms look like it is the average of D which causes diffusion, along with some corrective terms that have to do with the second Fourier coefficient.

Following the same derivation which we used to find (1.74) (with $V = 0$), we find the modified phase diffusion equation

$$\Phi_T = \frac{\Phi_{\phi\phi}}{r_c^2} \int D'(r)R(r)\, dr \tag{1.214}$$

where

$$R(r) = \frac{\exp\left(-\int \frac{u_1}{D''}\left(\frac{r}{r_c} - 1\right) dr\right)}{\int_{-\infty}^{\infty} \exp\left(-\int \frac{u_1}{D''}\left(\frac{r}{r_c} - 1\right) dr\right) dr} \tag{1.215}$$

The multiplier, $R(r)$, is just a weighting function over the radius which "averages" the diffusion, $D'(r)$. As can be seen in (1.215), it reduces to a Gaussian when D'' is constant. If we further assume that $D'' = 0$, then we may take this weight as tending to an impulse (δ-function). The denominator is just the normalizing factor necessary to make the integral of $R(r)$ equal to unity. We can interpret $R(r)$ as the distribution of oscillators in the radial direction. Stronger attraction to the limit cycle will cause $R(r)$ to peak more and have shorter width, whereas weaker attractions tend to produce wider smoother weighting functions.

We see that the overall diffusion then is a weighted sum of diffusions about the limit cycle. In general, solving for the phase diffusion with the weighted diffusion term is a rather hefty problem. However, if we specify the case when the weighting function is a δ-function (strong attraction to the limit cycle), we get the phase diffusion

$$\Phi_T = \frac{D'(r_c)}{r_c^2} \Phi_{\phi\phi} \tag{1.216}$$

which has phase noise

$$S_{vv}(\Delta\omega) \approx \frac{\frac{1}{2\pi} \int_0^{2\pi} \frac{1}{4} S_{ww} \cos^2\theta \, d\theta}{\Delta\omega^2} \tag{1.217}$$

This reduces to (1.75) when S_{ww} is constant, i.e., stationary.

A.1.4 FOURIER TRANSFORM

We want to find

$$\mathcal{F}\left[e^{-a|t|} \cos\omega_0 t\right] = \int_{-\infty}^{\infty} e^{-a|t|} e^{-i\omega t} \cos\omega_0 t \, dt \tag{1.218}$$

for $a > 0$. We start by calculating

$$\int_{-\infty}^{\infty} e^{-a|t|} e^{-i\omega t} \, dt = \int_0^{\infty} e^{-at} e^{-i\omega t} \, dt + \int_{-\infty}^{0} e^{at} e^{-i\omega t} \, dt \tag{1.219}$$

$$= \int_0^{\infty} e^{-at} e^{-i\omega t} \, dt + \int_0^{\infty} e^{-at} e^{i\omega t} \, dt \tag{1.220}$$

$$= \int_0^{\infty} e^{-(a+i\omega)t} \, dt + \int_0^{\infty} e^{-(a-i\omega)t} \, dt \tag{1.221}$$

$$= \frac{1}{a + i\omega} + \frac{1}{a - i\omega} \tag{1.222}$$

$$= \frac{2a}{a^2 + \omega^2} \tag{1.223}$$

Therefore,

$$\int_{-\infty}^{\infty} e^{-a|t|} e^{-i\omega t} \cos\omega_0 t \, dt = \int_{-\infty}^{\infty} e^{-a|t|} e^{-i\omega t} \left(\frac{e^{i\omega_0 t} + e^{-i\omega_0 t}}{2}\right) dt \tag{1.224}$$

$$= \frac{1}{2} \int_{-\infty}^{\infty} e^{-a|t|} e^{-i(\omega+\omega_0)t} \, dt$$

$$+ \frac{1}{2} \int_{-\infty}^{\infty} e^{-a|t|} e^{-i(\omega-\omega_0)t} \, dt \tag{1.225}$$

$$= \frac{a}{a^2 + (\omega+\omega_0)^2} + \frac{a}{a^2 + (\omega-\omega_0)^2} \tag{1.226}$$

We see that for ω close to ω_0,

$$\mathcal{F}\left[e^{-a|t|} \cos\omega_0 t\right] \approx \frac{a}{a^2 + \Delta\omega_0^2} \approx \frac{a}{\Delta\omega_0^2} \tag{1.227}$$

where $\Delta\omega_0 = \omega - \omega_0$ and it was assumed that $a \ll \Delta\omega_0$.

A.1.5 FOURIER TRANSFORM 2

To find the Fourier transform of (1.103), we consider

$$\mathcal{F}\left[e^{-a\frac{1}{\lambda}(|t|+\frac{1}{\lambda}(e^{-\lambda|t|}-1))}\right] = \int_{-\infty}^{\infty} e^{-a\frac{1}{\lambda}(|t|+\frac{1}{\lambda}(e^{-\lambda|t|}-1))} e^{-i\omega t} \, dt \tag{1.228}$$

where a is a positive constant. Breaking up the integral into two parts and rewriting the integrand into a form that can be integrated by parts,

$$= \int_0^{\infty} + \int_{-\infty}^{0} \tag{1.229}$$

$$= \int_0^{\infty} \frac{d}{dt} \left\{ e^{-a\frac{1}{\lambda}(t+\frac{1}{\lambda}(e^{-\lambda t}-1))} e^{-i\omega t} \right\} \frac{dt}{-\dfrac{a}{\lambda} + \dfrac{a}{\lambda} e^{-\lambda t} - i\omega}$$

$$+ \int_{-\infty}^{0} \frac{d}{dt} \left\{ e^{a\frac{1}{\lambda}(t-\frac{1}{\lambda}(e^{\lambda t}-1))} e^{-i\omega t} \right\} \frac{dt}{\dfrac{a}{\lambda} - \dfrac{a}{\lambda} e^{\lambda t} - i\omega} \tag{1.230}$$

$$= - \int_0^{\infty} e^{-a\frac{1}{\lambda}(t+\frac{1}{\lambda}(e^{-\lambda t}-1))} e^{-i\omega t} \frac{ae^{-\lambda t}}{\left(-\dfrac{a}{\lambda} + \dfrac{a}{\lambda} e^{-\lambda t} - i\omega\right)^2} \, dt + \frac{1}{i\omega}$$

$$- \int_{-\infty}^{0} e^{a\frac{1}{\lambda}(t-\frac{1}{\lambda}(e^{\lambda t}-1))} e^{-i\omega t} \frac{ae^{\lambda t}}{\left(\dfrac{a}{\lambda} - \dfrac{a}{\lambda} e^{\lambda t} - i\omega\right)^2} \, dt - \frac{1}{i\omega} \tag{1.231}$$

Repeating the same manipulation, we rewrite the equation as

$$= -\int_0^\infty \frac{d}{dt}\left\{ e^{-a\frac{1}{\lambda}(t+\frac{1}{\lambda}(e^{-\lambda t}-1))}e^{-i\omega t}e^{-\lambda t}\right\} \frac{a}{\left(-\frac{a}{\lambda}+\frac{a}{\lambda}e^{-\lambda t}-i\omega\right)^2} \frac{1}{-\frac{a}{\lambda}+\frac{a}{\lambda}e^{-\lambda t}-i\omega-\lambda}\, dt$$

$$-\int_{-\infty}^0 \frac{d}{dt}\left\{ e^{a\frac{1}{\lambda}(t-\frac{1}{\lambda}(e^{\lambda t}-1))}e^{-i\omega t}e^{\lambda t}\right\} \frac{a}{\left(\frac{a}{\lambda}-\frac{a}{\lambda}e^{\lambda t}-i\omega\right)^2} \frac{1}{\frac{a}{\lambda}-\frac{a}{\lambda}e^{\lambda t}-i\omega+\lambda}\, dt \quad (1.232)$$

$$=\frac{a}{\omega^2}\frac{1}{i\omega+\lambda}$$

$$+\int_0^\infty e^{-a\frac{1}{\lambda}(t+\frac{1}{\lambda}(e^{-\lambda t}-1))}e^{-i\omega t}e^{-\lambda t}\frac{d}{dt}\left\{ \frac{a}{\left(-\frac{a}{\lambda}+\frac{a}{\lambda}e^{-\lambda t}-i\omega\right)^2}\frac{1}{-\frac{a}{\lambda}+\frac{a}{\lambda}e^{-\lambda t}-i\omega-\lambda}\right\}\, dt$$

$$+\frac{a}{\omega^2}\frac{1}{-i\omega+\lambda}$$

$$+\int_{-\infty}^0 e^{a\frac{1}{\lambda}(t-\frac{1}{\lambda}(e^{\lambda t}-1))}e^{-i\omega t}e^{\lambda t}\frac{d}{dt}\left\{ \frac{a}{\left(\frac{a}{\lambda}-\frac{a}{\lambda}e^{\lambda t}-i\omega\right)^2}\frac{1}{\frac{a}{\lambda}-\frac{a}{\lambda}e^{\lambda t}-i\omega+\lambda}\right\}\, dt \quad (1.233)$$

$$\approx\frac{a}{\omega^2}\frac{2\lambda}{\lambda^2+\omega^2}, \qquad \omega\to\infty \quad\quad\quad (1.234)$$

where the last step comes because the integrands are rapidly varying for large ω, thereby making the integrals negligible when compared to the boundary terms. This is the method of stationary phase. Thus,

$$\mathcal{F}\left[e^{-a\frac{1}{\lambda}(|t|+\frac{1}{\lambda}(e^{-\lambda|t|}-1))}\cos\omega_0 t\right] = \int_{-\infty}^\infty e^{-a\frac{1}{\lambda}(|t|+\frac{1}{\lambda}(e^{-\lambda|t|}-1))}\cos\omega_0 t\, e^{-i\omega t} \quad (1.235)$$

$$\approx \frac{1}{(\omega+\omega_0)^2}\frac{a\lambda}{\lambda^2+(\omega+\omega_0)^2}$$

$$+\frac{1}{(\omega-\omega_0)^2}\frac{a\lambda}{\lambda^2+(\omega-\omega_0)^2} \quad\quad (1.236)$$

$$\approx \frac{1}{\Delta\omega^2}\frac{a\lambda}{\lambda^2+\Delta\omega^2} \quad\quad\quad (1.237)$$

where the second line comes from the asymptotic solutions found earlier and the last line is valid for ω close to ω_0. We defined $\Delta\omega=\omega-\omega_0$.

A.1.6   METHOD OF LAPLACE

The method of Laplace can be used to find asymptotic solutions to

$$I = \int_0^\infty h(t)e^{-\phi(t)}\,dt \tag{1.238}$$

where

$$\phi(t) = \frac{(t-2\pi k)^2}{4\delta\epsilon t} \tag{1.239}$$

and ϵ is considered small. Noting that the integrand contributes most to the integral when the exponent is largest, we seek out minima of $\phi(t)$ for $t \in [0,\infty)$. This occurs at $2\pi k$, which we denote by c from now on. Hence, it is easy to see that

$$\phi(c) = 0 \tag{1.240}$$

$$\phi'(c) = 0 \tag{1.241}$$

$$\phi''(c) = \frac{1}{4\pi k\delta\epsilon} \geq 0 \tag{1.242}$$

Expanding $\phi(t)$ about c,

$$\phi(t) = \frac{1}{2}(t-c)^2\phi''(c) + O(t^3) \tag{1.243}$$

Therefore,

$$I = \int_0^\infty h(t)e^{-\phi(t)}\,dt \tag{1.244}$$

$$\sim \int_{c-\epsilon'}^{c+\epsilon'} h(t)e^{-\phi(t)}\,dt \tag{1.245}$$

$$\sim \int_{c-\epsilon'}^{c+\epsilon'} h(c)\exp\left(-\frac{1}{2}(t-c)^2\phi''(c)\right)\,dt \tag{1.246}$$

$$\sim \int_{-\infty}^{\infty} h(c)\exp\left(-\frac{1}{2}(t-c)^2\phi''(c)\right)\,dt \tag{1.247}$$

where (1.245) comes from the fact that the contribution to the integral outside of the small region $[c-\epsilon', c+\epsilon']$ get exponentially smaller as $\epsilon \to 0$. In this small region,

$\phi(t)$ can be expanded as a Taylor series about c, giving (1.246). Extending the limits of integration now back to $(-\infty, \infty)$ in (1.247) is done because it is not very easy to find the integral of a gaussian over a subset of the real line, whereas integrating over the real line simply introduces exponentially small errors. Note that although the two integrands in (1.244) and (1.247) may differ significantly when far from c, their integrals (even over different limits) are close because each step only introduces exponentially small errors. Now evaluating (1.247),

$$I = \sqrt{\frac{2}{\phi''(c)}} \int_{-\infty}^{\infty} h(c) \, e^{-s^2} \, ds \qquad (1.248)$$

where we made the substitution

$$s^2 = \frac{1}{2}(t-c)^2 \phi''(c) \qquad (1.249)$$

Therefore,

$$I = \sqrt{\frac{2\pi}{\phi''(c)}} h(c) \qquad (1.250)$$

$$= 2\pi h(c)\sqrt{2k\delta\epsilon} \qquad (1.251)$$

when plugging in (1.242). Thus, it is now clear that (1.93) is

$$E(T) = \int_0^\infty \frac{1}{\sqrt{4\pi\delta\epsilon t}} \exp\left(-\frac{(t-2\pi k)^2}{4\delta\epsilon t}\right) \left(\frac{t}{2} + \pi k\right) dt \sim 2\pi k \qquad (1.252)$$

Similarly, (1.95) is

$$E(T^2) = \int_0^\infty \frac{1}{\sqrt{4\pi\delta\epsilon t}} \exp\left(-\frac{(t-2\pi k)^2}{4\delta\epsilon t}\right) \left(\frac{t^2}{2} + \pi kt\right) dt \sim 4\pi^2 k^2 \qquad (1.253)$$

Finding the variance, however, requires also expanding $h(t)$ as a Taylor series, since $h(c) = 0$ as can be seen by looking at the integral of (1.98),

$$\text{Var}(T) = \int_0^\infty \frac{1}{\sqrt{4\pi\delta\epsilon t}} \exp\left(-\frac{(t-2\pi k)^2}{4\delta\epsilon t}\right) \left(\frac{1}{2} + \frac{\pi k}{t}\right) (t-2\pi k)^2 \, dt \qquad (1.254)$$

Since $h(c) = h'(c) = 0$, the first non-zero term of $h(t)$ is $\frac{1}{2}h''(c)(t-c)^2$,

$$\text{Var}(T) \sim \sqrt{\frac{2}{\phi''(c)}} \int_{-\infty}^{\infty} \frac{h''(c)}{\phi''(c)} s^2 e^{-s^2} \, ds \tag{1.255}$$

where the same substitution (1.249) was made. Inserting

$$h''(c) = \sqrt{\frac{2}{\pi k}} \frac{1}{\sqrt{4\pi\delta\epsilon}} \tag{1.256}$$

into our expression along with (1.242), we get

$$\text{Var}(T) \sim 8k\delta\epsilon\sqrt{\pi} \int_{-\infty}^{\infty} s^2 e^{-s^2} \, ds \tag{1.257}$$

$$= 16k\delta\epsilon\sqrt{\pi} \int_{0}^{\infty} s^2 e^{-s^2} \, ds \tag{1.258}$$

$$= 8k\delta\epsilon\sqrt{\pi} \int_{0}^{\infty} u^{1/2} e^{-u} \, du \tag{1.259}$$

$$= 8k\delta\epsilon\sqrt{\pi}\, \Gamma\left(\frac{3}{2}\right) \tag{1.260}$$

$$= 4\pi k\delta\epsilon \tag{1.261}$$

where (1.258) comes from noticing that the integrand is symmetric about $s = 0$, and (1.259) makes the obvious substitution $u = s^2$. The definition of the gamma function is used to find (1.260) and (1.261).

Chapter 2

Subharmonic Frequency Entrainment

2.1 Frequency entrainment

Nonlinear oscillators also possess the interesting ability to couple with other oscillations. Speaking specifically, when an external driving oscillation is fed into a nonlinear oscillator at a frequency close to the nonlinear oscillator's natural frequency, it is sometimes possible to coerce the driven oscillator into oscillating at the same frequency as the external source. This effect is called frequency entrainment.

This effect was first noticed by the dutch physicist Christian Huygens in 1665. While sick and bed-ridden, he noticed how two pendulum clocks hanging on the same wall tended to oscillate at the same frequency. In a letter to his father, he described the phenomenon and called it the "sympathy of two clocks." This was the first documented incident of frequency entrainment, or injection-locking as it is sometimes

called. Since then, many occurrences of this bizarre phenomenon have been found to occur in other areas of life. Priests have long known that two organ pipes which resonated at close frequencies tended to sound as one tone, rather than beat like two. Biologists trekking through southeast Asia have explained the glowing of forests to the synchronized flashing of fireflies. The human sleep-wake cycle has been found to have a period slightly longer than the normal 24-hour cycle of the day, indicating that the sun does have a strong effect on the circadian rhythm of most people. In the laser field, lasing has been explained as the synchronization of emission of electrons. And last but not least, an electronic oscillator can be designed to lock to another oscillator, thus enabling frequency division as will be explained shortly.

Of course, not every oscillator locks to every other oscillator. There are limits, after all. The further the injected oscillator's frequency lies from the natural frequency of the driven oscillator, the greater the coupling must be. Coupling, in a very vague sense, is how "close" the two oscillators are, and usually depends on the amplitude of the driving oscillator. In general, frequency entrainment does occur both ways. In other words, when locked, both oscillators oscillate at the same frequency, which will be at a frequency in between both of their natural frequencies. However, most of the examples given have described oscillations in which one oscillator, the driving oscillator, is so steadfast that its frequency can be thought immutable. In cases like these, the strength of the coupling is affected by the amplitude of the driving oscillator. As a side note, one can say that grad students who don't follow "normal" waking hours are less susceptible to the effects of the sun. Perhaps a stronger star would regulate us.

Although most of the cited examples above describe 1:1 entrainment where the external forcing frequency is close to the natural frequency of the driven oscillator,

this need not be the case. We now know that rational-ratioed entrainment does occur. Exploiting this feature is what enables the phenomenon called injection-locked frequency division. Unlike direct 1:1 coupling, subharmonic 2:1 entrainment means that the driving oscillator locks to the second harmonic of the driven oscillator. The driven oscillator is designed to enhance the amount of second harmonic present to strengthen the coupling for 2:1 entrainment. Thus, when locked, the fundamental frequency of the driven oscillator will always be half the second harmonic, thus tracking half the driving oscillator's frequency. This is how 2:1 frequency division works.

We describe two methods to solving for the locking range of a 2:1 injection-locked divider. The first method uses the method of multiple scales, whereas the second method is based on the method of averaging.

2.2   Using the method of multiple scales

The basic idea behind the method of multiple scales, as demonstrated in the previous chapter, is the separation of the different processes occurring in the system through appropriate time scalings. In each particular scale, the other processes can be viewed as being *slow* or *fast*. In this way, it is possible to neglect the effects of the other processes by assuming their parameters to be constant, or rapidly varying (may be integrated out), thus isolating the desired process for further inspection, and hopefully, finding a solution.

We start with the normalized oscillator with small polynomial nonlinearity and external forcing.

$$\ddot{x} + x = \epsilon \left(\dot{x} + \delta \dot{x}^2 - \dot{x}^3 \right) + \gamma \cos \omega t \tag{2.1}$$

Intrinsic to this forced oscillator system are two different time scales. One is the scale associated with the oscillations. Another is the scale associated with the locking.

Usually, the former occurs on a much faster scale than the latter. Knowing this, we create two different time scalings, a *fast* time and a *slow* time. Creating the fast, $\xi = \omega t$, and slow, $\eta = \epsilon t$, time scales, we write

$$\dot{x} = x_\xi \omega + x_\eta \epsilon \tag{2.2}$$

$$\ddot{x} = x_{\xi\xi} \omega^2 + x_{\eta\eta} \epsilon^2 + 2\epsilon\omega x_{\eta\xi} \tag{2.3}$$

Rewriting (2.1) with this new scaling, we get

$$\omega^2 x_{\xi\xi} + \epsilon^2 x_{\eta\eta} + 2\epsilon\omega x_{\eta\xi} + x = \epsilon \left(x_\xi \omega + x_\eta \epsilon + \delta \left(x_\xi \omega + x_\eta \epsilon \right)^2 - \left(x_\xi + x_\eta \epsilon \right)^3 \right)$$
$$+ \gamma \cos \xi \tag{2.4}$$

Now expanding ω and x as perturbation series,

$$\omega = 2 + \epsilon k_1 + \cdots \tag{2.5}$$

$$x(\xi, \eta) = x_0(\xi, \eta) + \epsilon x_1(\xi, \eta) + \cdots \tag{2.6}$$

We expand ω about 2 since we are considering 2:1 entrainment. Collecting terms of the same order, we get the $O(1)$ equation,

$$x_{0\xi\xi} + \frac{1}{4} x_0 = \frac{1}{4} \gamma \cos \xi \tag{2.7}$$

which has solution

$$x_0 = A(\eta) \cos \frac{1}{2}\xi + B(\eta) \sin \frac{1}{2}\xi - \frac{1}{3} \gamma \cos \xi \tag{2.8}$$

where A and B are the "constants" of integration which are constant with respect to the fast time variable, ξ, but can depend on the slow time variable, η. To see the mechanism of locking occur, we need to go further and find the $O(\epsilon)$ equation,

$$x_{1\xi\xi} + \frac{1}{4} x_1 = -k_1 x_{0\xi\xi} - x_{0\eta\xi} + \frac{1}{2} x_{0\xi} + \delta x_{0\xi}^2 - 2 x_{0\xi}^3 \tag{2.9}$$

To solve this, we need to replace all occurrences of x_0 with the solution (2.8). First, we find

$$x_0 = A \cos \frac{1}{2}\xi + B \sin \frac{1}{2}\xi - \frac{1}{3}\gamma \cos \xi \tag{2.10}$$

$$x_{0\xi} = -\frac{1}{2}A \sin \frac{1}{2}\xi + \frac{1}{2}B \cos \frac{1}{2}\eta + \frac{1}{3}\gamma \sin \xi \tag{2.11}$$

$$x_{0\xi\xi} = -\frac{1}{4}A \cos \frac{1}{2}\xi - \frac{1}{4}B \sin \frac{1}{2}\eta + \frac{1}{3}\gamma \cos \xi \tag{2.12}$$

$$x_{0\eta\xi} = -\frac{1}{2}A' \sin \frac{1}{2}\eta + \frac{1}{2}B' \cos \frac{1}{2}\eta \tag{2.13}$$

Now, using (2.10)–(2.13) in (2.9), we get

$$x_{1\xi\xi} + \frac{1}{4}x_1 = \cos \frac{1}{2}\xi \left(\frac{Ak_1}{4} - \frac{B'}{2} + \frac{B}{4} - \frac{A}{6}\gamma\delta - \frac{3}{16}B(A^2 + B^2) - \frac{1}{6}B\gamma^2 \right)$$
$$+ \sin \frac{1}{2}\xi \left(\frac{Bk_1}{4} + \frac{A'}{2} - \frac{A}{4} + \frac{B}{6}\gamma\delta + \frac{3}{16}A(A^2 + B^2) + \frac{1}{6}A\gamma^2 \right)$$
$$+ \text{other terms} \tag{2.14}$$

Since we want nondivergent solutions, we remove secular terms by setting the coefficients of the resonant terms, $\cos \frac{1}{2}\xi$ and $\sin \frac{1}{2}\xi$, to 0. Thus,

$$\frac{Ak_1}{4} - \frac{B'}{2} + \frac{B}{4} - \frac{A}{6}\gamma\delta - \frac{3}{16}B(A^2 + B^2) - \frac{1}{6}B\gamma^2 = 0$$
$$\frac{Bk_1}{4} + \frac{A'}{2} - \frac{A}{4} + \frac{B}{6}\gamma\delta + \frac{3}{16}A(A^2 + B^2) + \frac{1}{6}A\gamma^2 = 0 \tag{2.15}$$

Rewriting as flow equations for A and B,

$$A' = -\frac{Bk_1}{2} + \frac{A}{2} - \frac{B\delta\gamma}{3} - \frac{3}{8}A(A^2 + B^2) - \frac{1}{3}A\gamma^2$$
$$B' = \frac{Ak_1}{2} + \frac{B}{2} - \frac{A\delta\gamma}{3} - \frac{3}{8}B(A^2 + B^2) - \frac{1}{3}B\gamma^2 \tag{2.16}$$

We now pause to remember that A and B are the amplitudes of the leading-order oscillations, as in (2.8). Thus, locking occurs when both of these "constants" have

settled. In other words, we are looking for the fixed point in the A–B plane. We get this by setting

$$A' = B' = 0 \qquad (2.17)$$

It is more illustrative to view this settling in polar coordinates, so we convert (A, B) into (r, θ) with

$$A = r \cos \theta$$

$$B = r \sin \theta$$

$$A' = r' \cos \theta - r\theta' \sin \theta \qquad (2.18)$$

$$B' = r' \sin \theta + r\theta' \cos \theta$$

Substituting into (2.16) and simplifying,

$$r' = \frac{r}{2} - \frac{r\delta\gamma}{3} \sin 2\theta - \frac{3}{8}r^3 - \frac{r\gamma^2}{3}$$

$$\theta' = \frac{k_1}{2} - \frac{\delta\gamma}{3} \cos 2\theta \qquad (2.19)$$

Thus, the fixed point (2.17) is found by setting

$$r' = \theta' = 0 \qquad (2.20)$$

The equations for the fixed point are then

$$0 = r_0 \left(\frac{1}{2} - \frac{\delta\gamma}{3} \sin 2\theta_0 - \frac{3}{8}r_0^2 - \frac{\gamma^2}{3} \right)$$

$$0 = \frac{k_1}{2} - \frac{\delta\gamma}{3} \cos 2\theta_0 \qquad (2.21)$$

where (r_0, θ_0) are the coordinates of the fixed point. However, the problem is not complete yet. We need to calculate the stability of each fixed point to determine whether the oscillations are locked. To determine the locking range, we need only find the points where a change of stability occurs. We look at linear stability, which is adequate if the fixed point is hyperbolic (Hartman-Grobman theorem [11]). Thus,

consider small excursions from the fixed point,

$$r = r_0 + \rho$$

$$\theta = \theta_0 + \phi$$

(2.22)

Substituting into (2.19), we get

$$\rho' = \frac{r_0}{2} + \frac{\rho}{2} - \frac{\delta\gamma}{3}(r_0 + \rho)(\sin 2\theta_0 + 2\phi\cos 2\theta_0)$$

$$- \frac{3}{8}(r_0^3 + 3r_0^2\rho) - \frac{\gamma^2}{3}(r_0 + \rho) + \cdots$$

(2.23)

$$\phi' = \frac{k_1}{2} - \frac{\delta\gamma}{3}\cos 2\theta_0 + \frac{2\delta\gamma}{3}\phi\sin 2\theta_0 + \cdots$$

where we dropped higher powers of ρ and ϕ. Using (2.21) to simplify,

$$\rho' = \frac{\rho}{2} - \frac{2\delta\gamma}{3}r_0\phi\cos 2\theta_0 - \frac{\delta\gamma}{3}\rho\sin 2\theta_0 - \frac{9}{8}r_0^2\rho - \frac{\gamma^2}{3}\rho$$

$$\phi' = \frac{2\delta\gamma}{3}\phi\sin 2\theta_0$$

(2.24)

Writing this in vector form,

$$\dot{\mathbf{z}} = \mathbf{A}\mathbf{z}$$

(2.25)

where

$$\mathbf{z} = \begin{bmatrix} \rho \\ \phi \end{bmatrix}$$

(2.26)

and

$$\mathbf{A} = \begin{bmatrix} \frac{1}{2} - \frac{\delta\gamma}{3}\sin 2\theta_0 - \frac{9}{8}r_0^2 - \frac{1}{3}\gamma^2 & -\frac{2\delta\gamma}{3}r_0\cos 2\theta_0 \\ 0 & \frac{2\delta\gamma}{3}\sin 2\theta_0 \end{bmatrix}$$

(2.27)

The fixed point is stable when

$$\text{tr}(\mathbf{A}) < 0$$

(2.28)

$$\det(\mathbf{A}) > 0$$

(2.29)

55

(see Appendix). Therefore, simplifying (2.27) using the equations for the fixed point (2.21),

$$
\mathbf{A} = \begin{bmatrix} -\dfrac{3}{4}r_0^2 & -r_0 k_1 \\ 0 & -\sqrt{\dfrac{\delta^2 \gamma^2}{9} - \dfrac{k_1^2}{4}} \end{bmatrix}
\tag{2.30}
$$

where we chose the negative square root to ensure that the inequalities (2.30) were true. The positive square root corresponds to the "flipped" solution, where θ_0 differs by π. This is the unstable configuration which does not lead to entrainment. We see that a change of stability occurs along the curve where $\det(\mathbf{A}) = 0$. Neglecting the trivial point, $r_0 = 0$, we find that locking happens above the curve

$$
\gamma^2 = \frac{9}{4\delta^2} k_1^2
\tag{2.31}
$$

Thus, we see that stronger injected signals have a greater chance of locking, as they broaden the frequency range in which locking is possible. This locking range is also enhanced by an increase in the second-order nonlinearity. Note that the absence of *any* second-order nonlinearity ($\delta = 0$) would make it impossible for 2:1 subharmonic entrainment to occur.

2.3 Using the method of averaging

The idea behind this perturbation method to calculating the locking range is to allow the constants of integration in the unperturbed solutions to vary. This variation will then account for the drift the oscillator undergoes as it locks to the external forcing. By watching how these "constants" vary, we are essentially rotating to the reference frame of the desired locked frequency and searching for conditions which make the "constants" settle.

Starting with the same equation (2.1) as in the previous section, but repeated

here for convenience,

$$\ddot{x} + x = \epsilon \left(\dot{x} + \delta \dot{x}^2 - \dot{x}^3 \right) + \gamma \cos \omega t \qquad (2.32)$$

Writing this as a system,

$$\dot{x} = y$$
$$\dot{y} = -x + \gamma \cos \omega t + \epsilon(y + \delta y^2 - y^3) \qquad (2.33)$$

We assume the solution takes on the form of the solution to the unperturbed ($\epsilon = 0$) system. Thus,

$$x = r \sin \left(\frac{\omega}{k} t + \theta \right) + B \cos \omega t$$
$$y = \frac{\omega}{k} r \cos \left(\frac{\omega}{k} t + \theta \right) - \omega B \sin \omega t \qquad (2.34)$$

where

$$B = \frac{\gamma}{1 - \omega^2} \qquad (2.35)$$

and k is the harmonic that the forcing frequency is trying to lock. Letting the parameters, r and θ, vary and plugging in (2.34) into (2.33),

$$\dot{x} = \frac{\omega}{k} r \cos(\ldots) - \omega B \sin \omega t \qquad (2.36)$$

$$= \dot{r} \sin(\ldots) + \frac{\omega}{k} r \cos(\ldots) + r \dot{\theta} \cos(\ldots) - \omega B \sin \omega t \qquad (2.37)$$

and

$$\dot{y} = -r \sin(\ldots) - B \cos \omega t + (1 - \omega^2) B \cos \omega t + \epsilon(y + \delta y^2 - y^3) \qquad (2.38)$$

$$= \frac{\omega}{k} \dot{r} \cos(\ldots) - \frac{\omega^2}{k^2} r \sin(\ldots) - \frac{\omega}{k} r \dot{\theta} \sin(\ldots) - \omega^2 B \cos \omega t \qquad (2.39)$$

where

$$(\ldots) = \left(\frac{\omega}{k} t + \theta \right) \qquad (2.40)$$

After some cancelations, we get

$$\dot{r} \sin(\ldots) + r \dot{\theta} \cos(\ldots) = 0 \qquad (2.41)$$

and

$$\frac{\epsilon\beta}{k^2}r\sin(\ldots) + \frac{\omega}{k}\dot{r}\cos(\ldots) - \frac{\omega}{k}r\dot{\theta}\sin(\ldots) = \epsilon(y + \delta y^2 - y^3) \tag{2.42}$$

where we made the definition

$$\epsilon\beta = k^2 - \omega^2 = O(\epsilon) \tag{2.43}$$

The definition (2.43) implies that we are looking at solutions where the forcing frequency, ω, is close to the kth multiple of the oscillator's natural frequency. This is for k:1 entrainment.

Using (2.41) and (2.42) to find the flow equations for r and θ,

$$\frac{\omega}{k}\dot{r} = \epsilon(y + \delta y^2 - y^3)\cos(\ldots) - \frac{\epsilon\beta}{k^2}r\sin(\ldots)\cos(\ldots)$$
$$-\frac{\omega}{k}r\dot{\theta} = \epsilon(y + \delta y^2 - y^3)\sin(\ldots) - \frac{\epsilon\beta}{k^2}r\sin^2(\ldots) \tag{2.44}$$

Now using the method of averaging, we write

$$\frac{\omega}{k}\dot{r} = \left\langle \epsilon(y + \delta y^2 - y^3)\cos(\ldots) - \frac{\epsilon\beta}{k^2}r\sin(\ldots)\cos(\ldots) \right\rangle$$
$$-\frac{\omega}{k}r\dot{\theta} = \left\langle \epsilon(y + \delta y^2 - y^3)\sin(\ldots) - \frac{\epsilon\beta}{k^2}r\sin^2(\ldots) \right\rangle \tag{2.45}$$

Simplifying (see Appendix),

$$\dot{r} = \epsilon\left(\frac{r}{2} + \frac{\delta\omega Br}{2}\sin 2\theta - \frac{3}{32}\omega^2 r^3 - \frac{3}{4}\omega^2 B^2 r\right)$$
$$\dot{\theta} = \epsilon\left(\frac{\delta\omega B}{2}\cos 2\theta + \frac{\beta}{4\omega}\right) \tag{2.46}$$

Again, setting $\dot{r} = \dot{\theta} = 0$, we get the equations for the fixed point

$$0 = r_0\left(1 + \delta\omega B\sin 2\theta_0 - \frac{3}{16}\omega^2 r_0^2 - \frac{3}{2}\omega^2 B^2\right)$$
$$0 = \delta\omega B\cos 2\theta_0 + \frac{\beta}{2\omega} \tag{2.47}$$

Expanding our coordinates about the fixed point as in (2.22), and plugging back into the averaged flow equations (2.46)

$$\dot{\rho} = \epsilon \left(\frac{\rho}{2} + \frac{\delta \omega B \rho}{2} \sin 2\theta_0 + \delta \omega B r_0 \phi \cos 2\theta_0 - \frac{9}{32} \omega^2 r_o^2 \rho - \frac{3}{4} \omega^2 B^2 \rho \right) \tag{2.48}$$

$$\dot{\phi} = -\epsilon \delta \omega B \phi \sin 2\theta_0$$

Writing this in vector form,

$$\mathbf{A} = \begin{bmatrix} \frac{1}{2} + \frac{\delta \omega B}{2} \sin 2\theta_0 - \frac{9}{32} \omega^2 r_0^2 - \frac{3}{4} \omega^2 B^2 & \delta \omega B r_0 \cos 2\theta_0 \\ 0 & -\delta \omega B \sin 2\theta_0 \end{bmatrix} \tag{2.49}$$

Again, recalling the conditions for linear stability, we look for

$$\text{tr}(\mathbf{A}) < 0 \tag{2.50}$$

$$\det(\mathbf{A}) > 0 \tag{2.51}$$

Plugging in (2.47) into (2.49), we get

$$\mathbf{A} = \begin{bmatrix} -\frac{3}{16} \omega^2 r_0^2 & -\frac{\beta r_0}{2\omega} \\ 0 & -\sqrt{\delta^2 \omega^2 B^2 - \frac{\beta^2}{4\omega^2}} \end{bmatrix} \tag{2.52}$$

where again, as in the previous section, we chose the negative square root which corresponds to the stable solution. Thus, we see that frequency entraiment occurs above the curve

$$B^2 = \frac{\beta^2}{4\delta^2 \omega^4} \tag{2.53}$$

We can rewrite (2.53) in a form similar to that found in the previous section (2.31). To do this, recall the definitions for B (2.35) and β (2.43), and define $\omega = 2 + \Delta \omega$ Then,

$$B^2 = \frac{\gamma^2}{(1 - \omega^2)^2} \approx \frac{\gamma^2}{9} \tag{2.54}$$

and

$$\epsilon^2\beta^2 = (4 - \omega)^2 \tag{2.55}$$

$$= 16 - 8\omega^2 + \omega^4 \tag{2.56}$$

$$\approx 16\Delta\omega^2 \tag{2.57}$$

where we kept terms only up to order $O(\Delta\omega^2)$ to make the last approximation. Thus, from (2.53),

$$\gamma^2 \approx \frac{9\Delta\omega^2}{4\delta^2\epsilon^2} \tag{2.58}$$

which is exactly what we got using the method of multiple scales (2.31) if we make the substitution $\Delta\omega = \epsilon k_1$.

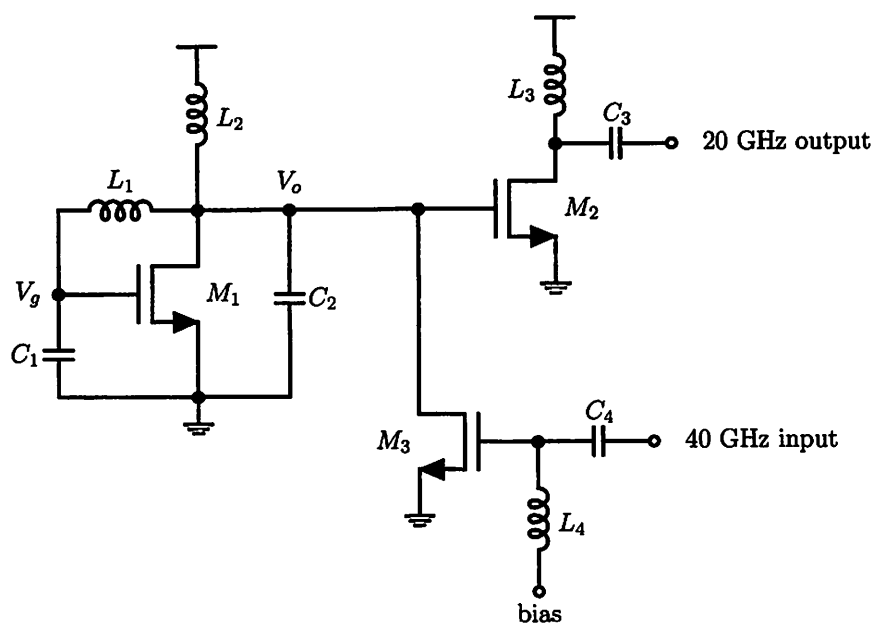## 2.4   2:1 Injection-locked frequency divider

Figure 2.1   40 GHz 2:1 injection-locked frequency divider.

The schematic for the 2:1 divider based on the Pierce oscillator topology is shown in Fig. 2.1. The differential equation describing this oscillator is

$$I_{L_1} + I_R + I_{L_2} = I(V_g, V_o) + C_2 \frac{d}{dt} V_o - I_{inj} \tag{2.59}$$

where $I(V_g, V_o)$ is the drain current flowing through transistor M_1, and I_{L_1} and I_{L_2} are currents flowing into node V_o through inductors L_1 and L_2, respectively. The resistance, R, models the finite Q of the inductor with I_R flowing into node V_o as well. The injected current is modeled by I_{inj}. If we make the approximation that C_2 and C_1 form a good capacitive transformer, then we can approximate the gate voltage, V_g, by

$$V_g \approx -kV_o \tag{2.60}$$

where

$$k = \frac{C_2}{C_1} \tag{2.61}$$

Assuming not much high-frequency current flows through L_2, which is a good approximation if this inductor behaves like a choke, we neglect I_{L_2} in our equation. Thus, we rewrite (2.59) as

$$-\frac{1}{L_1} \int (1+k)V_o \, dt - (1+k)\frac{V_o}{R} = I(V_o) + C_2 \frac{d}{dt} V_o - I_{inj} \tag{2.62}$$

Defining

$$q = \int V_o \, dt \tag{2.63}$$

we get,

$$\ddot{q} + \frac{1}{L_1 C_T} q = -\frac{1}{RC_T} \dot{q} - \frac{1}{C_2} I(\dot{q}) + \frac{1}{C_2} I_{inj} \tag{2.64}$$

where we defined

$$C_T = \frac{C_1 C_2}{C_1 + C_2} \tag{2.65}$$

$$= \frac{C_2}{1 + k} \tag{2.66}$$

Then nondimensionalizing time with

$$\frac{t}{\sqrt{L_1 C_T}} \to t \qquad (2.67)$$

(2.64) becomes

$$\ddot{q} + q = -\frac{\sqrt{L_1 C_T}}{R C_T}\dot{q} - \frac{L_1 C_T}{C_2}I(\dot{q}) + \frac{L_1 C_T}{C_2}I_{inj} \qquad (2.68)$$

Now, in order to get a differential equation in the form of (2.1), we need to be able to fit $I(\dot{q})$ to a cubic polynomial. Viewing simulations of the current flowing through our transistor, using (2.60) to relate the drain and gate voltages, we see in Fig. 2.2 that a cubic polynomial could be adequate in representing the nonlinearity. The bias voltages were set at $V_G = V_D = 0.5\,\text{V}$ to get the extracted curve.
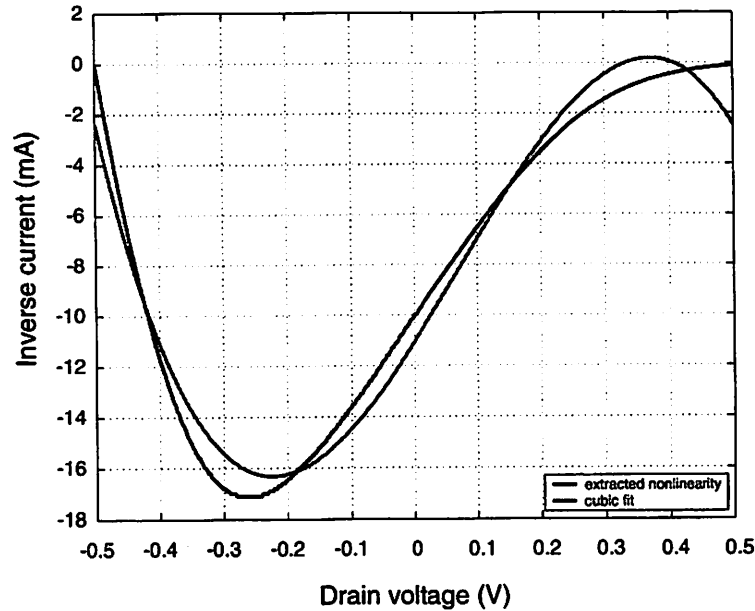

Figure 2.2 Polynomial fitting to current.

Approximating $I(V_o)$ with a third-order polynomial,

$$-I(V_o) = a_1 V_o + a_2 V_o^2 + a_3 V_o^3 \qquad (2.69)$$

62

we get,

$$-I(\dot{q}) = \frac{a_1}{\sqrt{L_1 C_T}}\dot{q} + \frac{a_2}{L_1 C_T}\dot{q}^2 + \frac{a_3}{(L_1 C_T)^{3/2}}\dot{q}^3 \qquad (2.70)$$

and so, we find

$$\ddot{q} + q = \frac{1}{Q}\left(\frac{R}{1+k}a_1 - 1\right)\dot{q} + \frac{a_2}{C_2}\dot{q}^2 + \frac{a_3}{C_2\sqrt{L_1 C_T}}\dot{q}^3 + \frac{L_1 C_T}{C_2}I_{inj} \qquad (2.71)$$

where

$$\frac{1}{Q} = \frac{1}{R}\sqrt{\frac{L_1}{C_T}} \qquad (2.72)$$

We now try to get (2.71) into the form of (2.1). Let

$$\epsilon = \frac{1}{Q}\left(\frac{R}{1+k}a_1 - 1\right) \qquad (2.73)$$

and nondimensionalize q with

$$\frac{q}{\sqrt{\frac{C_2 \epsilon}{-a_3}}(L_1 C_T)^{1/4}} \to q \qquad (2.74)$$

we find

$$\ddot{q} + q = \epsilon\left(\dot{q} + \frac{a_2}{\sqrt{-a_3}}\frac{(L_1 C_T)^{1/4}}{\sqrt{C_2 \epsilon}}\dot{q}^2 - \dot{q}^3\right) + \gamma\cos(\omega t) \qquad (2.75)$$

where

$$\gamma = \frac{L_1 C_T}{C_2}\sqrt{\frac{-a_3}{C_2 \epsilon}}\frac{I_{inj}}{(L_1 C_T)^{1/4}} \qquad (2.76)$$

Thus, we get the coefficient for the second-order nonlinearity, δ, to be

$$\frac{1}{\delta} = \frac{\sqrt{C_2 \epsilon}}{a_2}\frac{\sqrt{-a_3}}{(L_1 C_T)^{1/4}} \qquad (2.77)$$

Plugging this into (2.31), we find the relation between the locking range and the strength of the injected signal for the Pierce oscillator (in denormalized coordinates)

$$I_{inj} = \frac{3}{2}\frac{C_2^2}{a_2\sqrt{L_1 C_T}}\Delta\omega \qquad (2.78)$$

63

As a first-order approximation, we relate the injected voltage to the injected current through

$$I_{inj} = g_m V_{inj} \tag{2.79}$$

Thus, the final form for the locking range–injected voltage relation is

$$V_{inj} = \frac{3}{2} \frac{C_2^2}{a_2 g_m \sqrt{L_1 C_T}} \Delta\omega \tag{2.80}$$

Note how no mention of the resistor, R, appears in (2.80). This is because R, which is linked to Q, is more of a relative quantity which determines the percentage of the locking bandwidth to the center frequency. Since we are only looking at absolute frequency offsets from the center, it seems more likely that the absolute bandwidth depend on the actual value of the capacitances.

We plot (2.80) in Fig. 2.3, along with the curve given using [35]

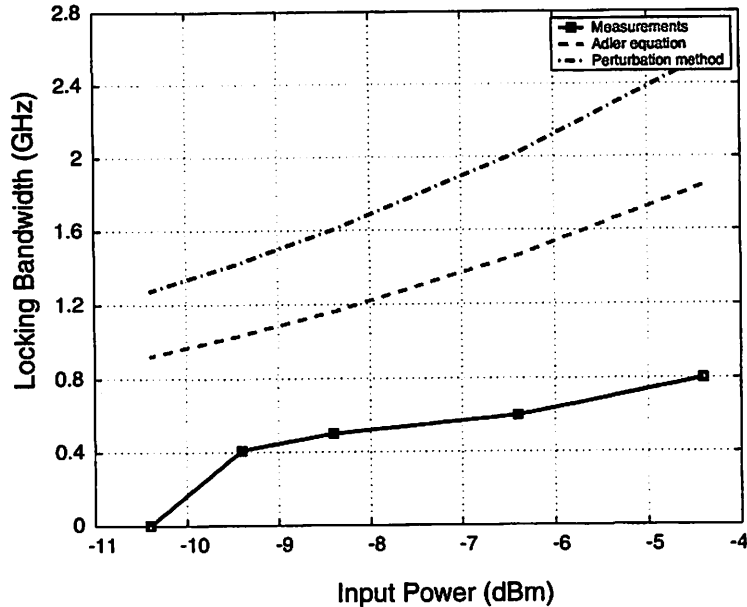$$V_{inj} = \frac{2Q V_{osc}}{\omega_0} \Delta\omega \tag{2.81}$$

Figure 2.3   Comparison of predicted locking ranges to measured results.

where V_{osc} is the oscillation amplitude in the tank. Based off of simulations, it was found that the amplitude of the injected voltage, V_{inj}, was approximately equal to the amplitude of the same frequency signal in the tank, hence the induced tank voltage was approximated to be equal to V_{inj} in (2.81). Note that in the two previous equations, $\Delta\omega$ is the one-sided frequency deviation allowable to achieve frequency entrainment. The actual locking bandwidth is double this value.

We see that the matching between (2.80) and measured results is not that close. There are several possible reasons for this. The first one is the difficulty in being able to accurately extract the actual power at the injected port. With the injection port not matched to 50 Ω, the actual power going into the gate of the transistor M_3 is less than what was calculated with. Another possible explanation for the deviation is the possibility that modeling the resonator as a lumped inductor in parallel with a capacitor might not be exactly right, as the resonator was constructed as a transmission line (details of the implementation of this oscillator can be found in the Appendix). Also, the value used for g_m as a first-order approximation were taken at the bias values. It is not necessarily true that the current injected at 40 GHz will be exactly $g_m V_{inj}$. More than likely, it will be less. All of these lead to less power being applied to the tank, thus lowering the locking bandwidth.

The discrepancy between Adler's equation and measured results is probably due to the inappropriate use of his equation in this case. Adler [35] derived his locking range for 1:1 coupling, which is not true in frequency dividers. When coupling at the natural frequency of the oscillator, the injected signal needs only to be of $O(\epsilon)$ in strength [23]. Subharmonic entrainment, on the other hand [16] [23], requires the signal to be larger. Thus, an approximation which Adler made, which is valid for his derived result, that $V_{inj} \ll V_{osc}$ is no longer applicable to injection-locked dividers. Extensions to his

work [34] [33] have been made to account for coupling in injection-locked dividers, but those results model the subharmonic frequency entrainment phenomenon as coupling to harmonics present in the oscillator. The main problem with this view is that the fundamental is still present and drastically affects the behavior of the system. Thus, it is still not valid to assume that the injected signal may be small.

APPENDIX

A.2.1   LINEAR STABILITY OF DYNAMICAL SYSTEMS

Consider the linear system

$$\dot{\mathbf{y}} = \mathbf{A}\mathbf{y} \tag{2.82}$$

The fixed point of this system can be found by setting

$$0 = \mathbf{A}\mathbf{y}_0 \tag{2.83}$$

Now consider small excursions from the fixed point, $\mathbf{y}_0$, by defining

$$\mathbf{y} = \mathbf{y}_0 + \mathbf{z} \tag{2.84}$$

Then (2.82) becomes

$$\dot{\mathbf{z}} = \mathbf{A}\mathbf{y}_0 + \mathbf{A}\mathbf{z} \tag{2.85}$$

$$= \mathbf{A}\mathbf{z} \tag{2.86}$$

This basically shows that we do not lose any generality by considering the fixed point to be at the origin. For this system to be stable, all the eigenvalues of $\mathbf{A}$ must be negative. For the two-dimensional case, we can express the matrix $\mathbf{A}$ as

$$\mathbf{A} = \begin{bmatrix} a & b \\ c & d \end{bmatrix} \tag{2.87}$$

The characteristic equation is

$$\det(\lambda \mathbf{I} - \mathbf{A}) = \begin{vmatrix} \lambda - a & -b \\ -c & \lambda - d \end{vmatrix} \tag{2.88}$$

$$= \lambda^2 - (a + d)\lambda + ad - bc \tag{2.89}$$

$$= \lambda^2 - \text{tr}(\mathbf{A}) + \det(\mathbf{A}) \tag{2.90}$$

$$= 0 \tag{2.91}$$

The two eigenvalues are

$$\lambda_{1,2} = \frac{1}{2} \left(\text{tr}(\mathbf{A}) \pm \sqrt{\text{tr}^2(\mathbf{A}) - 4\det(\mathbf{A})} \right) \tag{2.92}$$

Because we know the eigenvalues solve the characteristic equation, we can also write

$$0 = (\lambda - \lambda_1)(\lambda - \lambda_2) \tag{2.93}$$

$$= \lambda^2 - (\lambda_1 + \lambda_2)\lambda + \lambda_1\lambda_2 \tag{2.94}$$

Comparing to (2.90), we find

$$\text{tr}(\mathbf{A}) = \lambda_1 + \lambda_2 \tag{2.95}$$

$$\det(\mathbf{A}) = \lambda_1\lambda_2 \tag{2.96}$$

Hence, for stable systems, the trace has to be negative and the determinant has to be positive. The stability criteria are then

$$\text{tr}(\mathbf{A}) < 0 \tag{2.97}$$

$$\det(\mathbf{A}) > 0 \tag{2.98}$$

We can also say more about the type of stability by looking at eigenvalues (2.92). A complex eigenvalue with nonzero imaginary part contains oscillations about the fixed point. If the real part is negative, the trajectory spirals into the fixed point. If the

real part is positive, the trajectory spirals outward. In the dynamical systems field, these fixed points are called stable and unstable foci, respectively. If the eigenvalue contains no imaginary terms, negative and positive real parts correspond to stable and unstable nodes, respectively. Eigenvalues with zero real part, on the other hand, require further inspection. If the system truly is linear, such as (2.82), then a purely imaginary eigenvalue indicates that the trajectory of small excursions from the fixed point tend to produce oscillations which neither decay nor grow. Care must be taken, however, when trying to apply this to a linearized nonlinear system. The stability of a nonlinear system is equivalent to the stability of the linearized system *only* for hyperbolic systems, i.e., systems which have no eigenvalues with zero real parts. Otherwise, things get more complicated and more advanced techniques would have to be employed.

The regions of different stability types can be plotted in the $tr(\mathbf{A})$–$det(\mathbf{A})$ plane as in Fig. 2.4. In this plot, regions colored in gray denote instability. Systems which fall into region I have fixed points which are unstable nodes. The fixed points of region II systems are unstable foci. Region III corresponds to saddle-point type fixed points (one stable eigenvalue and one unstable eigenvalue). Region IV corresponds to stable foci, and region V is for stable nodes.

A.2.2 METHOD OF AVERAGING

The principle idea behind the method of averaging is exploiting the fact that the velocity field is small to be able to integrate out the time variable. Consider systems of the form

$$\dot{\mathbf{x}} = \epsilon \mathbf{f}(\mathbf{x}, t, \epsilon) \qquad (2.99)$$

where f has period T in t, and is $O(1)$. The velocity field, $\dot{\mathbf{x}}$, will then be $O(\epsilon)$, making
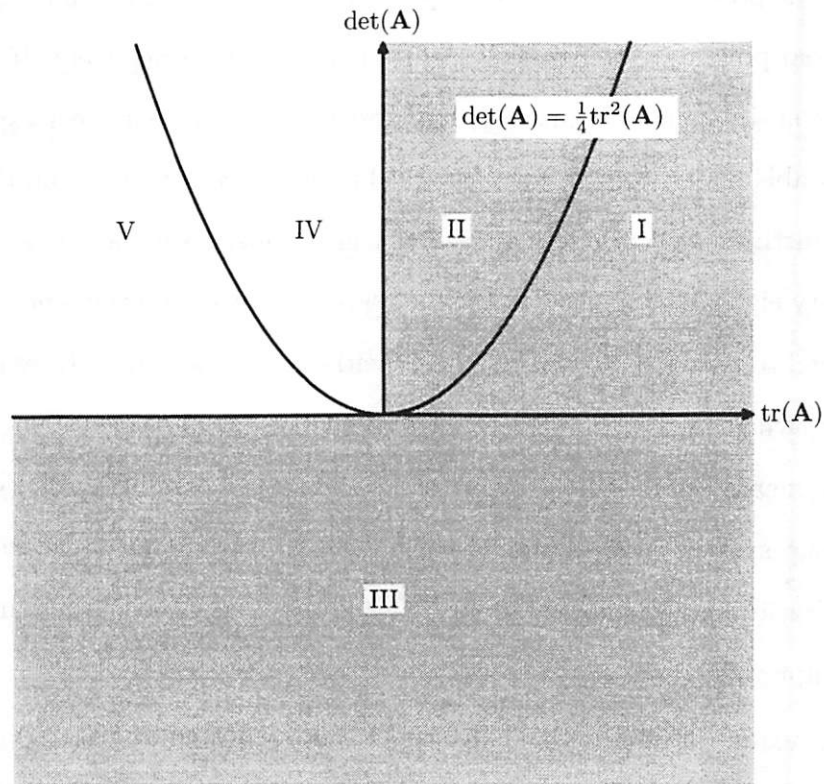
Figure 2.4 Regions of stability.

it seem plausible that we might be able to hold $\mathbf{x}$ constant in a time integral. That is exactly what the averaging theorem takes advantage of. It states

Averaging Theorem [11]. There exists a change of coordinates $\mathbf{x} = \mathbf{y} + \epsilon \mathbf{w}(\mathbf{y}, t, \epsilon)$ under which (2.99) becomes

$$\dot{\mathbf{y}} = \epsilon \frac{1}{T} \int_0^T \mathbf{f}(\mathbf{y}, t, 0)\, dt + \epsilon^2 \mathbf{f}_1(\mathbf{y}, t, \epsilon) \qquad (2.100)$$

where $\mathbf{f}_1$ is of period T in t.

In other words, if we find a solution, $\mathbf{y}(t)$, which solves the *averaged* equation,

$$\dot{\mathbf{y}} = \epsilon \frac{1}{T} \int_0^T \mathbf{f}(\mathbf{y}, t, 0)\, dt \qquad (2.101)$$

69

with $|\mathbf{x}_0 - \mathbf{y}_0| < \epsilon$ at time $t = 0$, then the solutions will be ϵ-close, i.e., $|\mathbf{x}(t) - \mathbf{y}(t)| < \epsilon$ for $t \sim 1/\epsilon$.

The averaged equation (2.101) is sometimes written

$$\dot{\mathbf{y}} = \epsilon \langle \mathbf{f}(\mathbf{y}, t, \epsilon) \rangle \tag{2.102}$$

where it is clear that the average is being taken over the period T in t and that $\epsilon = 0$ in the integral. Note also that the integral can be taken over any shifted version of the interval $[0, T]$.

A.2.3 CALCULATED AVERAGES

From (2.34),

$$y = \frac{\omega r}{k} \cos(\ldots) - \omega B \sin \omega t \tag{2.103}$$

$$y^2 = \left(\frac{\omega r}{k}\right)^2 \cos^2(\ldots) + \omega^2 B^2 \sin^2 \omega t - 2\frac{\omega^2 B r}{k} \cos(\ldots) \sin \omega t \tag{2.104}$$

$$y^3 = \left(\frac{\omega r}{k}\right)^3 \cos^3(\ldots) - \omega^3 B^3 \sin^3 \omega t - 3\left(\frac{\omega r}{k}\right)^2 \omega B \cos^2(\ldots) \sin \omega t$$
$$+ 3\frac{\omega^3 B^2 r}{k} \sin^2 \omega t \cos(\ldots) \tag{2.105}$$

remembering that

$$(\ldots) = \left(\frac{\omega}{k}t + \theta\right) \tag{2.106}$$

We calculate some averages to facilitate the computation of the averaged equation. Besides the obvious ones,

$$\langle \sin(\ldots) \cos(\ldots) \rangle = 0 \tag{2.107}$$

$$\langle \sin^2(\ldots) \rangle = \langle \cos^2(\ldots) \rangle = \frac{1}{2} \tag{2.108}$$

we find

$$\langle \sin(\ldots)\cos^2(\ldots)\rangle = \frac{1}{2}\langle \sin(\ldots)(1+\cos(\omega t+2\theta))\rangle \tag{2.109}$$

$$= 0 \tag{2.110}$$

$$= \langle \cos(\ldots)\sin^2(\ldots)\rangle \tag{2.111}$$

and

$$\langle \sin^3(\ldots)\rangle = \frac{1}{2}\langle \sin(\ldots)(1-\cos(\omega t+2\theta))\rangle \tag{2.112}$$

$$= 0 \tag{2.113}$$

$$= \langle \cos^3(\ldots)\rangle \tag{2.114}$$

where we used $k=2$. We also find

$$\langle \sin^2(\ldots)\sin\omega t\rangle = \frac{1}{2}\langle (1-\cos(\omega t+2\theta))\sin\omega t\rangle \tag{2.115}$$

$$= \frac{1}{4}\sin 2\theta \tag{2.116}$$

Similarly,

$$\langle \sin^2(\ldots)\cos\omega t\rangle = -\frac{1}{4}\cos 2\theta \tag{2.117}$$

$$\langle \cos^2(\ldots)\sin\omega t\rangle = -\frac{1}{4}\sin 2\theta \tag{2.118}$$

$$\langle \cos^2(\ldots)\cos\omega t\rangle = \frac{1}{4}\cos 2\theta \tag{2.119}$$

Therefore,

$$\langle y\sin(\ldots)\rangle = \langle -\omega B\sin\omega t\sin(\ldots)\rangle = 0 \tag{2.120}$$

$$\langle y\cos(\ldots)\rangle = \frac{\omega r}{2k} = \frac{\omega r}{4} \tag{2.121}$$

$$\langle y^2\sin(\ldots)\rangle = \left\langle \omega^2 B^2\sin^2\omega t\sin(\ldots) - 2\frac{\omega^2 Br}{k}\cos(\ldots)\sin(\ldots)\sin\omega t\right\rangle \tag{2.122}$$

$$= \left\langle \frac{\omega^2 B^2}{2}(1-\cos 2\omega t)\sin(\ldots) - \frac{\omega^2 Br}{k}\sin(\omega t+2\theta)\sin\omega t\right\rangle \tag{2.123}$$

$$= -\frac{\omega^2 Br}{4}\cos 2\theta \tag{2.124}$$

$$\langle y^2 \cos(\ldots)\rangle = \left\langle \frac{\omega^2 B^2}{2}(1 - \cos 2\omega t)\cos(\ldots) + \frac{\omega^2 Br}{4}\sin 2\theta \right\rangle \quad (2.125)$$

$$= \frac{\omega^2 Br}{4}\sin 2\theta \quad\quad\quad\quad (2.126)$$

$$\langle y^3 \sin(\ldots)\rangle = \left\langle -\omega^3 B^3 \sin^3 \omega t \sin(\ldots) - \frac{3}{2}\frac{\omega^3 Br^2}{k^2}\cos(\omega t + 2\theta)\sin \omega t \sin(\ldots) \right\rangle (2.127)$$

$$= \left\langle \frac{\omega^3 B^3}{2}\sin \omega t \cos 2\omega t \sin(\ldots) \right\rangle \quad\quad\quad (2.128)$$

$$= 0 \quad\quad\quad\quad (2.129)$$

$$\langle y^3 \cos(\ldots)\rangle = \left\langle \frac{3}{8}\left(\frac{\omega r}{k}\right)^3 - \frac{\omega^3 B^3}{2}\sin \omega t(1 - \cos 2\omega t)\cos(\ldots) \right.$$

$$- \frac{3}{2}\frac{\omega^3 Br^2}{k^2}(1 + \cos(\omega t + 2\theta))\sin \omega t \cos(\ldots)$$

$$\left. + \frac{3}{4}\frac{\omega^3 B^2 r}{k}(1 - \cos 2\omega t)(1 + \cos(\omega t + 2\theta)) \right\rangle \quad (2.130)$$

$$= \left\langle \frac{3}{8}\left(\frac{\omega r}{k}\right)^3 + \frac{3}{4}\frac{\omega^3 B^2 r}{k} \right\rangle \quad\quad (2.131)$$

$$= \frac{3}{64}\omega^3 r^3 + \frac{3}{8}\omega^3 B^2 r \quad\quad\quad (2.132)$$

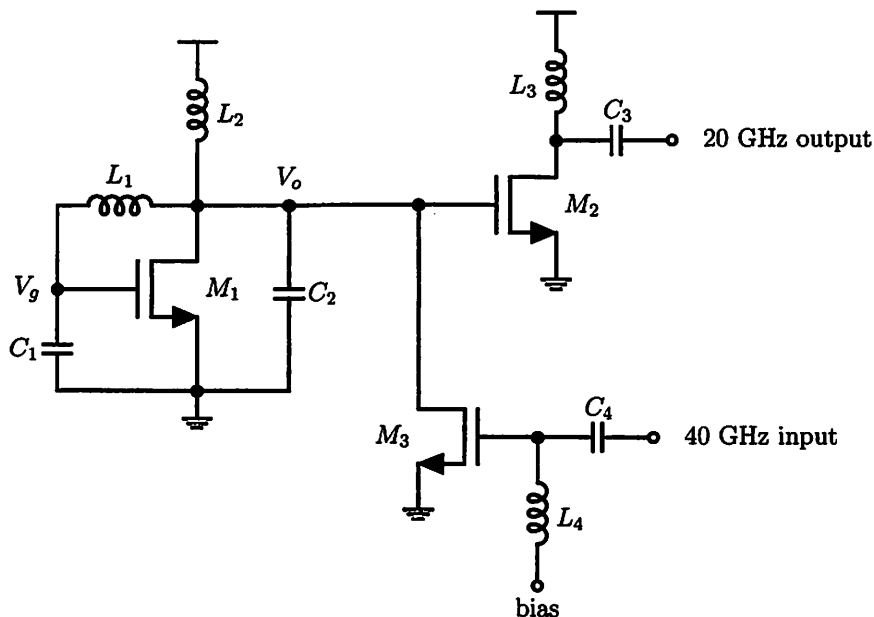## A.2.4 IMPLEMENTING A 40 GHZ 2:1 INJECTION-LOCKED FREQUENCY DIVIDER

Figure 2.5 Injection-locked divider.

This design of a 40-GHz 2:1 injection-locked frequency divider was completed in a standard 0.13-μm CMOS process. It consists mainly of a grounded source Pierce oscillator based on M_1 which has current injected directly into the tank via transconductor M_3. An output stage consisting of transistor M_2 is used to provide sufficient gain and isolation between the oscillator and the test equipment.

The Pierce oscillator was chosen because of its favored grounded source topology. This reduces bulk modulation and provides for better matching to extracted models. The ring resonator L_1 was built as a transmission line which looped between the drain and source of M_1. L_2 was designed to behave more or less like a choke, although it is not entirely open at those frequencies. The nominal frequency of this oscillator is 21.3 GHz. It was designed to operate at about 20 GHz. As shown in this chapter,

it is possible for a nonlinear oscillator to lock to an injected signal at a harmonic of the oscillator's natural frequency. This signal does not even have to be injected at a specific point. By simply impressing a strong enough signal in the main resonator, the nonlinearities of the oscillator will cause the overall oscillator's behavior to be affected. Thus, injection was achieved by inserting current directly into the tank through a current transconductor, M_3. The injected signal's frequency was chosen to come in at 40 GHz, making this a 2:1 frequency divider. An output stage was placed to provide the necessary gain to drive the 50-Ω load of the spectrum analyzer. It also provides some gain.

Since this circuit operates at a high frequency, transmission lines were viable alternatives to the harder-to-characterize spiral inductors. Hence, all of the inductors in this circuit were implemented as coplanar transmission lines. Specifically, the resonator which consists of L_1, C_1, and C_2, is a ring connecting the drain of M_1 to the gate. Underpasses were placed regularly to maintain good grounds on both sides of the coplanar transmission lines to prevent moding. This is especially important for the ground plane *inside* the ring because it has no other connection to the main power ground. A minimum distance of 50 μm between adjacent transmission lines was maintained to minimize coupling.

Heavy use of bypass capacitors helped stabilize biases and power to keep the circuit clean. They were also placed as close as possible to the desired end of the transmission lines to prevent extra "uncounted" lengths of transmission line from disturbing the operation of the circuit. In the same vein, components were spaced as closely as possible to minimize parasitics, especially in the core oscillator. Coupling capacitors were implemented as finger capacitors to minimize area while still providing good overall Q.
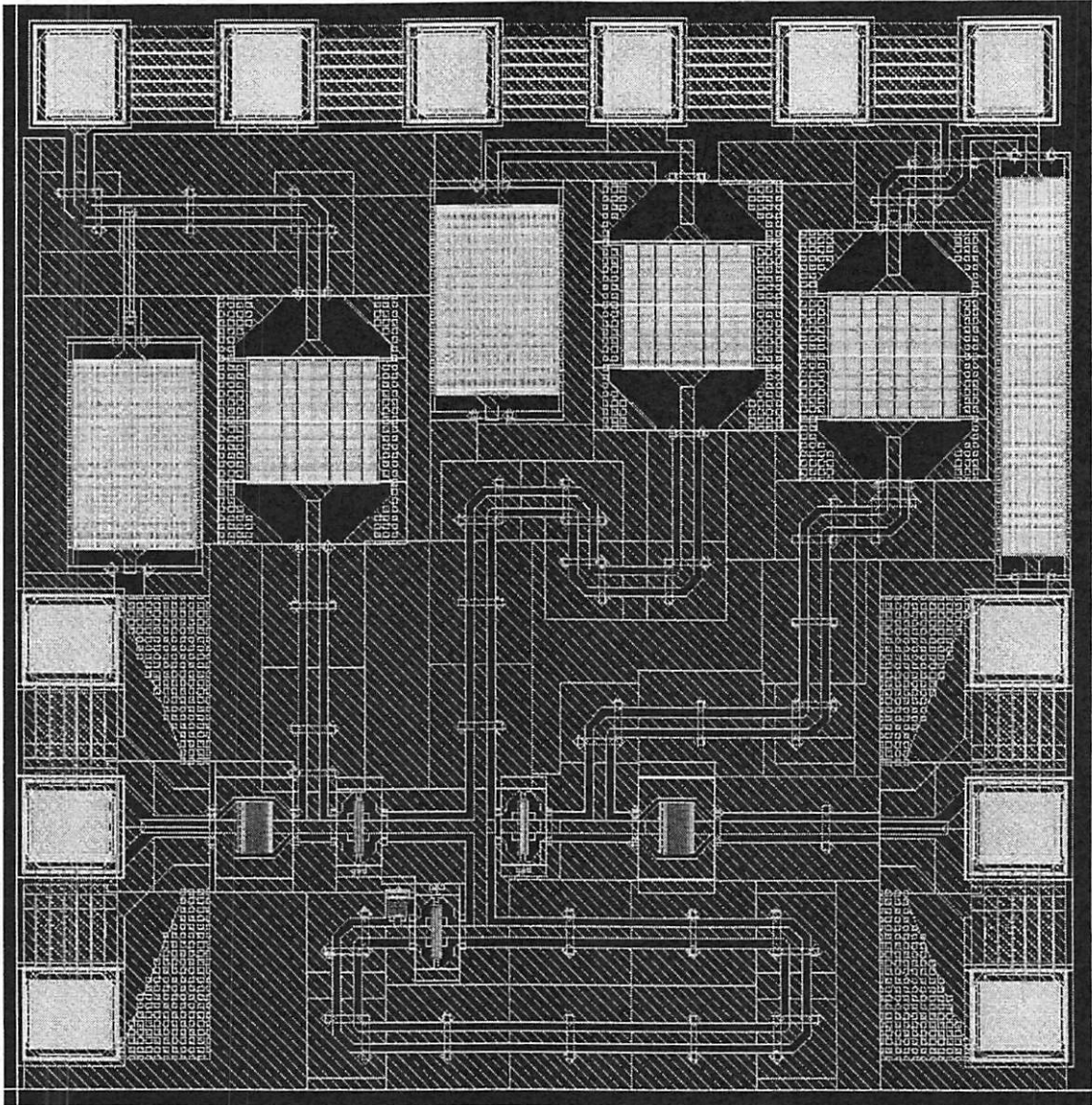
Figure 2.6 Chip layout.

Chip measurements were taken on a probe station using GSG (Ground–Signal–Ground) probes. An image of the chip layout is shown in Fig. 2.6. Note how most of the space between circuit components was filled with a metal ground plane. This is to minimize resistive paths between points that need a good ground. However, what may not be clearly visible in such a small image is the abundance of holes in

the metal. Most modern copper-metal processes require slotting to hold the metal in place. This chip was tested using a network analyzer to provide the injected signal, and an HP 8365E spectrum analyzer to determine locking.

Concluding Remarks

This thesis described a method to modeling oscillators and solving the associated problems of phase noise and injection-locking using perturbation theory. Since most oscillators tend to be nonlinear, finding explicit solutions for many of their properties can prove to be difficult without a computer. Perturbation theory is an asymptotic theory, which decomposes hard problems into simple ones with "corrections," that can be used to find good approximate analytical solutions to many problems, even nonlinear ones. For this reason, we chose to explore the possibility of using perturbation theory to solving two of the harder problems concerning electronic oscillators: phase noise and injection-locking. Even if exact solutions are not the end goal, being able to rigorously formulate an approximate solution has benefits in shedding more light on the underlying mechanism which generates phase noise or causes an oscillator to lock.

One of the main techniques of perturbation theory used is the method of multiple scales, which involves generating multiple scalings to separate out the effects of different processes. Specifically, in oscillators, one would generate two time scales, a fast time and a slow time, to isolate the effects of fast periodic motion from those of the slower system drifts which result in phase diffusion or frequency lock.

Another major theme to this thesis is the focus on finding a different way to view oscillator noise. Borrowing elements from the statistical physics arena, we take a particle diffusion approach to describing noise. By observing that a random walk

describes the accumulated sum of independent increments, we were able to gain valuable insight into proposing a model for oscillators and then formulating a diffusion equation for a noisy oscillator. The main idea is to rehash the problem of trying to solve for the properties of one noisy oscillator into the analogous problem of solving for the concentration density of oscillators having a certain property. In other words, we want to be looking for the *probability density* of oscillators. By considering an ensemble of possible oscillators, we formulated an advection-diffusion equation to model the evolution of the probability density in state space. The resulting advection-diffusion equation models the deterministic forces exerted on the oscillator with the advection (drift) term, while the random disturbances are handled by the diffusion term.

As was shown in this thesis, we can formulate the advection-diffusion equation and reduce it to a simpler phase diffusion equation for the case when the oscillator is weakly nonlinear, i.e., nearly sinusoidal oscillations. By converting to a rotating frame, we isolated the fast and slow time scales and applied a perturbation expansion which resulted in a reduced advection-diffusion equation. By solving for the impulse response (Green function) for this PDE, we found the probability of a certain transition (going from one state to another) at a given time. This can be used to find the autocorrelation function. The spectral density (Fourier transform of autocorrelation function) would then give phase noise when divided by the power of the steady-state signal. By taking the diffusion to be constant, we were able to find closed-form expressions for the phase noise. We also found quadrature solutions for the case when the noise was cyclostationary (diffusion is periodic about the limit cycle).

Interestingly, by considering the cyclostationary case, we found that the diffusion had more of an effect when the attraction to the limit cycle was weak. The reason comes from the fact that the magnitude of the phase advection is smallest on the

limit cycle (when in the rotated frame). In fact, it is zero. This is because the rotating frame rotates with the oscillator. Thus, weaker attractions to the limit cycle will tend to leave the distribution of oscillators spread widely about the limit cycle where they may be pushed forwards or backwards in phase. However, stronger attractions to the limit cycle keep the concentration of oscillators close to the limit cycle where the phase advection is small. This leads to the interesting conclusion that stronger nonlinearities, which result in stronger attraction, give lower phase noise. Although this may seem contradictory to circuit designers familiar with the phase noise performance of ring oscillators (a type of relaxation oscillator), it is not without explanation. Although the ring oscillator does have stronger attraction to its limit cycle *most* of the time, there are periods of fast transition which have weaker attraction. The attraction is so weak in this transition region that the overall phase noise ends up exceeding those found in sinusoidal oscillators for most cases. Thus, if it were possible to design for a tighter grip (stronger attraction) in the transition region, it might be possible to design a low-phase-noise ring oscillator.

Our solution also showed that the diffusion only affected the overall phase noise at certain key points in the cycle. Thus, by designing our oscillator such that the injected noise is minimized at certain points, we can reduce phase noise.

Looking at the big picture, we see that phase noise is generated through the diffusive nature of particle motion. Thus, we can also state that making the system more sluggish (i.e., through increasing capacitance in a parallel-tank oscillator or inductance in a series tank), would result in lower noise. However, we should not forget that the phase noise is always reported relative to the power of the signal, and changing these components could affect the limiting amplitude.

Applying our methods to the case of injection-locking, we considered the oscillator

in a frame rotating at the desired *lock* frequency in state space. The fast time was used to describe the fast periodic oscillations while slow time was used to trace out the trajectories of the oscillator in this rotating frame. We then used a perturbation expansion to look for fixed points in this space. The presence of a fixed point meant that the oscillator was not moving relative to the rotating frame and had thus achieved frequency synchronicity with the injected signal. A lock frequency of half the injected signal's frequency was used for our analysis of 2:1 injection-locked dividers. For this specific type of injection-locking, we found that the ability to lock depended on the magnitude of the second-order nonlinearity. In other words, larger second-order nonlinearties led to larger locking ranges for the same injected power.

Finally, as with all work, the work in this thesis is not complete. There is much to be done in this area. One possible extension would be to look at how the locking range of an injection-locked divider is affected by noise. By combining ideas from the two main chapters of this thesis, we can form a new model to describe our new problem and solve it using similar methods. Another possible extension is the analysis of the strongly nonlinear oscillator and finding corresponding phase diffusion expressions. Because of the drastic change in behavior between the slow and fast regions of the relaxation oscillator, we believe this problem will involve use of singular perturbation theory to extend our current methods. Going outside the realm of oscillators, we can use dynamical systems theory coupled with a particle diffusion view to model noise in systems that have state. This could range from problems dealing with stateful power amplifiers, to control theory motion planning problems, or perhaps even solving quantum mechanical problems! Alas, we do not have the time to look at every possible outgrowth of research coming out of this work. And, as everything must come to an end—this thesis is not an exception—we end here. Happy perturbing!

References

[1] J. D. Cole. *Perturbation Methods in Applied Mathematics.* Blaisdell, 1968.

[2] J. C. Neu. *Ma 204 Lecture Notes.* personal handouts, 1999.

[3] C. M. Bender and S. A. Orszag. *Advanced Mathematical Methods for Scientists and Engineers.* Springer-Verlag, 1999.

[4] A. van der Ziel. *Noise in Solid State Devices and Circuits.* Wiley, 1986.

[5] D. C. Lee. "Analysis of Jitter in Phase-Locked Loops," *IEEE Transactions on Circuits and Systems II*, Vol. 49, pp. 704–711, November 2002.

[6] S. Strogatz. *Sync: The Emerging Science of Spontaneous Order.* Theia, 2003.

[7] S. Strogatz. *Nonlinear Dynamics and Chaos.* Westview, 1994.

[8] S. Strogatz. *The Mathematical Structure of the Human Sleep-Wake Cycle.* Springer-Verlag, 1986.

[9] I. Percival and D. Richards. *Introduction to Dynamics.* Cambridge University Press, 1982.

[10] H. L. Pécseli. *Fluctuations in Physical Systems.* Cambridge University Press, 2000.

[11] J. Guckenheimer and P. Holmes. *Nonlinear Oscillations, Dynamical Systems, and Bifurcations of Vector Fields.* Springer-Verlag, 1983.

[12] A. A. Andronov and C. E. Chaikin. *Theory of Oscillations.* Princeton University Press, 1949.

[13] P. Fang, K. K. Hung, P. K. Ko, and C. Hu. "Hot-Electron-Induced Traps Studied Through the Random Telegraph Noise," *IEEE Electron Device Letters*, Vol. 12, pp. 273–275, June 1991.

[14] K. K. Hung, P. K. Ko, C. Hu, and Y. C. Cheng. "Random Telegraph Noise of Deep-Submicrometer MOSFET's," *IEEE Electron Device Letters*, Vol. 11, pp. 90–92, February 1990.

[15] K. K. Hung, P. K. Ko, C. Hu, and Y. C. Cheng. "A Unified Model for the Flicker Noise in Metal-Oxide-Semiconductor Field-Effect Transistors," *IEEE Transactions on Electron Devices*, Vol. 37, pp. 654–665, March 1990.

[16] J. K. Hale. *Ordinary Differential Equations*. Wiley, 1969.

[17] B. B. Mandelbrot. *Multifractals and 1/f Noise: Wild Self-Affinity in Physics*. Springer-Verlag, 1998.

[18] C. Kittel and H. Kroemer. *Thermal Physics*. W. H. Freeman and Company, 1980.

[19] W. Feller. *An Introduction to Probability Theory and Its Applications*. Wiley, 1950.

[20] G. F. Lawler. *Introduction to Stochastic Processes*. Chapman & Hall, 1995.

[21] B. Razavi. *RF Microelectronics*. Prentice Hall, 1998.

[22] T. H. Lee. *The Design of CMOS Radio-Frequency Integrated Circuits*. Cambridge University Press, 1998.

[23] R. Rand. *Nonlinear Vibrations*. http://www.tam.cornell.edu/randdocs/nlvibe45.pdf, 2003.

[24] J. Doob et al. *Noise & Stochastic Processes*. Dover Publications, 1954.

[25] B. Razavi. "A Study of Phase Noise in CMOS Oscillators," *IEEE J. Solid-State Circuits*, Vol. 31, pp. 331–343, March 1996.

[26] A. Hajimiri and T. H. Lee. "A General Theory of Phase Noise in Electrical Oscillators," *IEEE J. Solid-State Circuits*, Vol. 33, pp. 179–194, February 1998.

[27] A. Hajimiri and T. H. Lee. "Corrections to "A General Theory of Phase Noise in Electrical Oscillators"," *IEEE J. Solid-State Circuits*, Vol. 33, pp. 928, June 1998.

[28] D. Ham and A. Hajimiri. "Virtual Damping and Einstein Relation in Oscillators," *IEEE J. Solid-State Circuits*, Vol. 38, pp. 407–418, March 2003.

[29] A. Demir, A. Mehrotra, and J. Roychowdhury. "Phase noise in oscillators: A unifying theory and numerical methods for characterization," *IEEE Trans. Circuits Systems I*, Vol. 47, pp. 655–674, May 2000.

[30] D. B. Leeson. "A simple model of feedback oscillator noise spectrum," *Proc. IEEE*, Vol. 54, pp. 329–330, Feb. 1966.

[31] S. J. Farlow. *Partial Differential Equations for Scientists and Engineers*. Dover, 1993.

[32] R. Haberman. *Elementary Partial Differential Equations*. Prentice Hall, 1983.

[33] S. Verma, H. R. Rategh, and T. H. Lee. "A Unified Model for Injection-Locked Frequency Dividers," *IEEE J. Solid-State Circuits*, Vol. 38, pp. 1015–1027, June 2003.

[34] H. R. Rategh and T. H. Lee. "Superharmonic Injection-Locked Frequency Dividers," *IEEE J. Solid-State Circuits*, Vol. 34, pp. 813–821, June 1999.

[35] R. Adler. "A Study of Locking Phenomena in Oscillators," *Proceedings of the I.R.E. and Waves and Electrons*, Vol. , pp. 351–357, June 1946.

Colophon

This document was typeset using Plain TeX and a "thesis" macro package created by the author on a Linux operating system. Text editing was done in vim, the improved vi editor. Paragraphs were typeset using the included Computer Modern Roman fonts (CMR) at 12 point with double spacing. Chapter, section, subsection headings were typset using Century Gothic font (converted from the Windows Truetype font collection). Figures were created using Metapost. Text in the figures were typset by the TeX engine. Plots were generated in MATLAB. Simulation data taken from Cadence/Spectre were exported as text then imported into MATLAB for plotting. The PDF version was created using dvips with the embedded fonts option.